Florida State University
Department of Meteorology
Technical Note No. 66-7

ACOUSTIC-GRAVITY WAVES IN THE EARTH'S ATMOSPHERE

I. The General Nature of Acoustic-Gravity Waves

II. Acoustic-Gravity Wave Ducting in the Atmosphere by Vertical Temperature Structure

by

John C. Gille

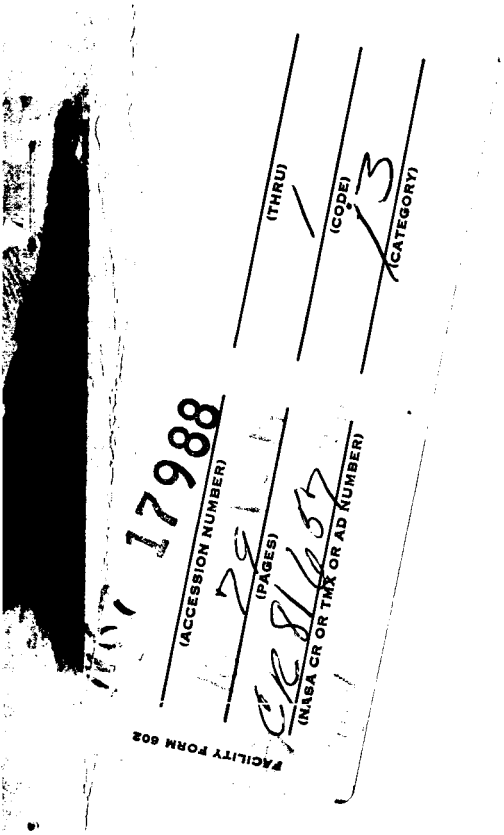

Lectures in the NATO Advanced Study Institute
on the topic
Movements and Turbulence of the Atmosphere
Between 30 and 120 km.

Held at Lindau on Lake Constance, W. Germany
September 19-30, 1966.

GPO PRICE $ _____

CFSTI PRICE(S) $ _____

Hard copy (HC) 3.00

Microfiche (MF) .65

ff 653 July 65

Partially supported by NASA Grant NSG-173, NSF Grant NSF GP 2371
and Office of Naval Research Contract Nonr 266(70).

December 1966

Florida State University

Department of Meteorology

Technical Note No. 66-7

Acoustic-Gravity Waves in the Earth's Atmosphere

I. The General Nature of Acoustic-Gravity Waves

II. Acoustic-Gravity Wave Ducting in the Atmosphere by Vertical Temperature Structure

by

John C. Gille

Lectures in the NATO Advanced Study Institute
on the topic
Movements and Turbulence of the Atmosphere
Between 30 and 120 km.

Held at Lindau on Lake Constance, W. Germany
September 19-30, 1966

Partially supported by NASA Grant NSG-173, NSF Grant NSF GP 2371 and Office of Naval Research Contract Nonr 266(70).

December 1966

Foreword

The motions observed in the earth's atmosphere display spatial and temporal scales which range from those for sound waves to those of the large-scale standing planetary waves. The same may be expected to be true of the atmospheres of other planets. To date, considerable effort has been expended on the largest scale circulations of other planets, but apparently much less attention has been paid to smaller scale motions, such as acoustic and internal-gravity waves.

In a preliminary step to the study of these phenomena in other atmospheres, where additional physical processes may be important, the present state of understanding of these waves in the earth's atmosphere was reviewed. An invitation to present two lectures on "Atmospheric Gravity Waves" to the NATO Advanced Study Institute on "Atmospheric Motions and Turbulence Between 30-120 km" held at Lindau on Lake Constance, W. Germany, September 19-30, 1966 was the occasion for writing down these summaries of several aspects of the problem.

These reviews are thus a concise statement of our present understanding, and a starting point for considerations of similar phenomena in the atmospheres of other planets.

These treatments are each self-contained, with separate pagination and bibliographies. For the convenience of the reader, a colored sheet has been inserted between them to facilitate opening to the second paper.

The preparation of these papers was primarily supported by NASA Grant NSG-173, for which I am very grateful. Previously unpublished material shown in the second paper resulted from studies supported by the National Science Foundation under Grant NSF GP 2371 and Office of Naval Research Contract Nonr 266(70).

I would like to thank Professor S. L. Hess for his encouragement in this work, and Professor R. L. Pfeffer for interesting me in this problem, unpublished material and physical insights.

John C. Gille

The General Nature of Acoustic-Gravity Waves

1. Introduction

In lectures today and tomorrow, we shall be speaking of the nature, propagation and ducting of infrasonic waves in the terrestrial atmosphere. Clearly, in two to three hours we cannot go into great mathematical detail. We will, therefore, attempt to do three things:

1. To see the basic mathematics and physics upon which the results are based;
2. To develop a physical feeling for the processes going on, and
3. To discuss qualitatively the results of numerical calculations, so that we may understand their implications.

I hope that with this broad overview of an area of intriguing but difficult problems, some of you will be sufficiently interested to turn to the references and fill in the details which we must here omit.

2. The Perturbation Equations

To develop the basic equations, let us consider a fluid initially at rest, and stratified in the vertical direction. We assume that the wave amplitudes are small compared to the wavelength, so that the equations of motion may be linearized. Also, we will neglect the effects of viscosity and thermal transfer, whether conductive or radiative. Since we are looking for length scales much less than the radius of the earth, and time scales much less than a day, we will neglect curvature and rotation.

We introduce the following symbols:

x, y, z	rectangular coordinates, z vertical
u, v, w	velocities in directions x, y, z, of perturbation order
$\rho_0(z), \rho_1$	basic and perturbation density
$p_0(z), p_1$	basic and perturbation pressure
$n_0(z), n_1$	basic and perturbation entropy.

The basic equations are developed by Eliassen and Kleinschmidt (1957).

We have the equations of

1) Momentum

$$\rho \frac{\vec{Dv}}{Dt} = - \nabla p + \rho \vec{g} \qquad \text{(Euler's equations)}$$

which becomes with our assumptions

$$\frac{dp_0}{dz} = - g\rho_0 \qquad \text{(Hydrostatic equation)} \qquad (1)$$

as the only zeroth order equation, and

$$\rho_0 \frac{\partial u}{\partial t} = - \frac{\partial p_1}{\partial x} \tag{2}$$

$$\rho_0 \frac{\partial w}{\partial t} + g\rho_1 = - \frac{\partial p_1}{\partial z} \tag{3}$$

2) Continuity

$$\frac{D\rho}{Dt} + \rho \nabla \cdot \vec{V} = 0$$

which yields

$$\frac{\partial \rho_1}{\partial t} + w \frac{\partial \rho_0}{\partial z} + \rho_0 \left(\frac{\partial u}{\partial x} + \frac{\partial w}{\partial z}\right) = 0; \quad \text{and} \tag{4}$$

3) Entropy conservation (adiabatic motion)

$$\frac{D\eta}{Dt} = 0$$

which becomes

$$\frac{\partial \eta_1}{\partial t} + w \frac{\partial \eta_0}{\partial z} = 0 . \tag{5}$$

To this we add the equation of state

$$p = \rho RT \tag{6}$$

where R = gas constant for air

T = temperature.

The state of a pure fluid can be specified by any two of the four variables ρ, p, η and temperature T. Thus

$$dp = \left(\frac{\partial p}{\partial \rho}\right)_\eta d\rho + \left(\frac{\partial p}{\partial \eta}\right)_\rho d\eta$$

Now

$$\left(\frac{\partial p}{\partial \rho}\right)_\eta = c^2 = \frac{\gamma P}{\rho} = \gamma RT$$

where

c = (adiabatic) sound velocity

$\gamma = c_p/c_v$

In the stratified equilibrium state,

$$\frac{dp_0}{dz} = - g\rho_0 = c_0^2 \frac{d\rho_0}{dz} + \gamma_0 \frac{d\eta_0}{dz} \tag{7}$$

while for small perturbation from this state

$$p_1 = c_0^2 \rho_1 + Y_0 \eta_1$$

and for adiabatic motion

$$\frac{\partial p_1}{\partial t} = c_0^2 \frac{\partial \rho_1}{\partial t} + Y_0 \frac{\partial \eta_1}{\partial t} \tag{8}$$

We can get rid of the entropy terms by combining 5, 7, and 8 to find

$$\frac{\partial p_1}{\partial t} = c_0^2 \frac{\partial \rho_1}{\partial t} - w \left[- g\rho_0 - c_0^2 \frac{\partial \rho_0}{\partial z} \right] \tag{9}$$

The perturbation density can be removed with (4) to give

$$\frac{\partial p_1}{\partial t} = w g \rho_0 - \rho_0 c_0^2 \left(\frac{\partial u}{\partial x} + \frac{\partial w}{\partial z} \right) \tag{10}$$

Finally, taking $\partial/\partial t$ of 2 and 3, we can get rid of the perturbation pressure, and are left with

$$\rho_0 \frac{\partial^2 u}{\partial t^2} = - g\rho_0 \frac{\partial w}{\partial x} + \frac{\partial}{\partial x} \left[\rho_0 c_0^2 \left(\frac{\partial u}{\partial x} + \frac{\partial w}{\partial z} \right) \right] \tag{11}$$

$$\rho_0 \frac{\partial^2 w}{\partial t^2} = g\rho_0 \frac{\partial u}{\partial x} + \frac{\partial}{\partial z} \left[\rho_0 c_0^2 \left(\frac{\partial u}{\partial x} + \frac{\partial w}{\partial z} \right) \right] \tag{12}$$

This derivation has followed that of Tolstoy (1936) (Appendix). They are also derived in Lamb (1945), in Eckart (1960), and many other places.

We shall look for solutions of the form

$$u = U(z)\, e^{i(kx-\omega t)}$$

$$w = W(z)\, e^{i(kx-\omega t)}$$

where k is the horizontal wave number

ω is the angular frequency

t is the time

Let us also suppress the zero subscript of c and ρ which will be taken hereafter to be the basic state.

On substitution in (11), we find

$$U = ik \left(\frac{c^2 W' - gW}{k^2 c^2 - \omega^2} \right) \tag{13}$$

where $\frac{d}{dz}$ is indicated by a prime, and from (12)

$$W'' + \frac{d}{dz} \ln \frac{\rho}{\frac{\omega^2}{c^2} - k^2} W' + \left[\frac{\omega^2}{c^2} - k^2 - \frac{k^2}{\omega^2} g \frac{d}{dz} \left(\ln \frac{\rho}{\frac{\omega^2}{c^2} - k^2} \right) - \frac{k^2 g^2}{\omega^2 c^2} \right] W = 0 \qquad (14)$$

We may note immediately that for ω large this reduces to the acoustic wave equation, while gravity effects enter in terms important for small ω.

Both coefficients depend on gradients of density and sound velocity. The latter are most important for the high frequency range. We can get a great deal of insight by assuming c = constant.

Then

$$W'' + \frac{d}{dz} (\ln \rho) W' + \left\{ \frac{\omega^2}{c^2} - k^2 + \frac{k^2}{\omega^2} \left[- g \frac{d}{dz} \ln \rho - \frac{g^2}{c^2} \right] \right\} W = 0 \qquad (15)$$

The term in square brackets has a particular explanation.

3. The Väisälä Frequency

Consider a single element of fluid, contained within a flexible, insulating membrane, and displaced vertically from its equilibrium position. When released, its motion will obey the equation

$$\rho \frac{\partial^2 \zeta}{\partial t^2} = - g \Delta \rho \qquad (1)$$

where ζ is the vertical distance from equilibrium and $\Delta\rho$ is the difference between internal and external density. $\Delta\rho = \Delta\rho$ (internal) $-\Delta\rho$ (environment) where $\Delta\rho$ (environment) is the change of density experienced simply because of motion in a stratified fluid. For an incompressible fluid we would have

$$\Delta\rho = - \Delta\rho \text{ (environment)} = -\zeta \frac{d\rho}{dz} . \qquad (2)$$

$\Delta\rho$ (internal) is due to the compressibility of the fluid within the membrane. Since the pressure is the same inside and out,

$$\Delta p \text{ (internal)} = \zeta \frac{dp_0}{dz} \qquad (3)$$

which, by virtue of 2.2 and 2.5 may be written

$$c^2 \Delta\rho \text{ (internal)} = - \zeta\rho\, g \tag{4}$$

Combining (1), (2), and (4)

$$\frac{\partial^2 \zeta}{\partial t^2} + \left[- g \frac{d}{dz} \ln \rho - \frac{g^2}{c^2} \right] \zeta = 0 \tag{5}$$

When the term in brackets is greater than zero*, simple harmonic motion will result, with

$$N^2 = - g \left[\frac{d}{dz} \ln \rho + \frac{g}{c^2} \right] \tag{6}$$

as the angular frequency. This is the Väisälä frequency, sometimes called the Brunt frequency. Clearly, it must be relevant for gravity waves.

4. Waves in an Infinite, Isothermal Atmosphere.

An equation of the form of 2.15 may be transformed in a standard manner [see Tolstoy (1963), Sect. 4] which in this case is

$$W = \rho^{-1/2} h \tag{1}$$

to reduce 2.15 to the form

$$h'' + n^2 h = 0 \tag{2}$$

where

$$n^2 = \frac{\omega^2}{c^2} - k^2 + \frac{k^2}{\omega^2} N^2 - \frac{1}{4} \left(\frac{d}{dz} \ln \rho \right)^2 - \frac{1}{2} \frac{d^2}{dz^2} \ln \rho \tag{3}$$

is seen to be a vertical wave number.

We shall sometimes find it convenient to make the additional assumption (equivalent to an isothermal atmosphere) that

$$\rho = \rho_0 e^{-z/H} = e^{-2\nu z} \tag{4}$$

where ρ_0 is the density at the origin of z, H is the scale height,

$$H = \frac{RT}{g} = \frac{c^2}{\gamma g}$$

---

*Stability against convective overturnings requires $N^2 > 0$.

and ν is a wave number characteristic of the stratification

$$\nu = \frac{1}{2H} = \frac{\gamma g}{2c^2}$$

With these approximations, (3) becomes

$$n^2 = \frac{\omega^2}{c^2} - k^2 + \frac{k^2}{\omega^2} N^2 - \nu^2 \qquad (5)$$

These assumptions are rather unrealistic, since N and ν vary considerably in the atmosphere. However, consideration of this model will provide us with physical insight which will be helpful in considering more realistic situations.

There are three separate effects in the equation for n^2:

(1) Compressibility, which enters in terms ω^2/c^2 and g^2/c^2. Incompressibility corresponds to $c = \infty$.

(2) Stratification: $\frac{d}{dz} \ln \rho$, $\frac{d^2}{dz^2} \ln \rho$. These terms vanish in homogeneous atmospheres.

(3) Gravity. This enters only in the definition of N^2.

Let us start with a simple case, and add complexity.

4.1 Incompressible, homogeneous case. ($c = \infty$, $\nu = 0$, $g \neq 0$)

Equation (5) becomes $n^2 = -k^2$. Thus $h \propto e^{\pm nz}$, an exponential. No real propagating wave system exists without boundaries. These are the gravity waves at an air-water interface, for example.

4.2 Compressible, homogeneous case, without gravity. ($c \neq \infty$, $\nu = 0$, $g = 0$)

$$n^2 = \frac{\omega^2}{c^2} - k^2 \qquad (6)$$

Thus h and w obey the acoustic wave equation, and since

$$\frac{\omega^2}{k^2 + n^2} = \frac{\omega^2}{K^2} = c^2 = \text{constant}, \qquad (7)$$

wave propagation is isotropic and non-dispersive.

4.3 Density stratified, compressible fluids, with g = 0. ($c \neq \infty$, $\nu \neq 0$)

In our isothermal atmosphere with constant scale height, (5) becomes

$$k^2 + n^2 = \frac{\omega^2}{c^2} - \nu^2$$

or

$$\omega_a^2 = c^2 (k^2 + n^2 + \nu^2)$$

Because of the symmetry between k and n, propagation is again isotropic, but note that for $\omega^2 < \nu^2 c^2$ unattenuated propagation is not possible. This frequency

$$\omega_0 = \nu c = \frac{\gamma g}{2c} \propto T^{-1/2} \qquad (9)$$

forms a low frequency cut off to these waves. Since they approach the acoustic equation at high frequencies

$$k^2 + n^2 >> \nu^2$$

these are acoustic type waves.

This cut off ω_0 is a resonant frequency for propagating waves, characteristic of a distributed mass - spring system.

We may graph this result in the ω - K plane as shown in Figure 1 (after Tolstoy, 1963). (Plotting ω vs k would be similar.) Note that the slope of a line from the origin to a point on the curve is $V = \omega/K$, the phase velocity, and is given by $V = \omega/K = c\ (1 - \omega_0^2/\omega^2)^{-1/2}$. Since the slope changes for different ω, the propagation is dispersive.

Of greater interest than the phase velocity is the group velocity

$$U(K) = \frac{d\omega}{dK} = c \left(1 - \frac{\omega_0^2}{\omega^2}\right)^{1/2}$$

the velocity with which the energy is propagated. It is, of course, the slope of the ω-K curve. As $\omega \to \omega_0$, $V \to \infty$ but $U \to 0$.

The cut-off frequency ω_0 may easily be calculated using

$c = 3.3 \cdot 10^4$ cm/sec,

$H = 8 \cdot 10^5$ cm, to be

$\omega_0 = .02$ sec^{-1}, corresponding to

$P_0 = \frac{2\pi}{\omega_0} = 5$ minutes.

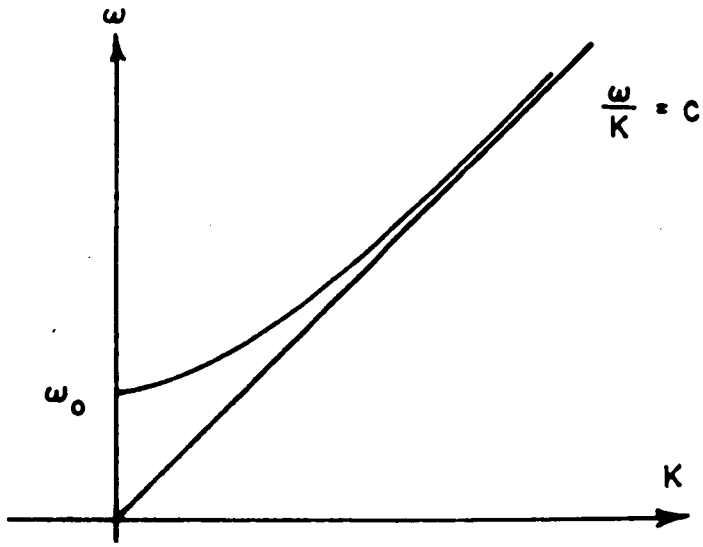

Fig. 1. Dispersion of acoustic waves in an infinite medium with density stratification. (After Tolstoy, 1963)

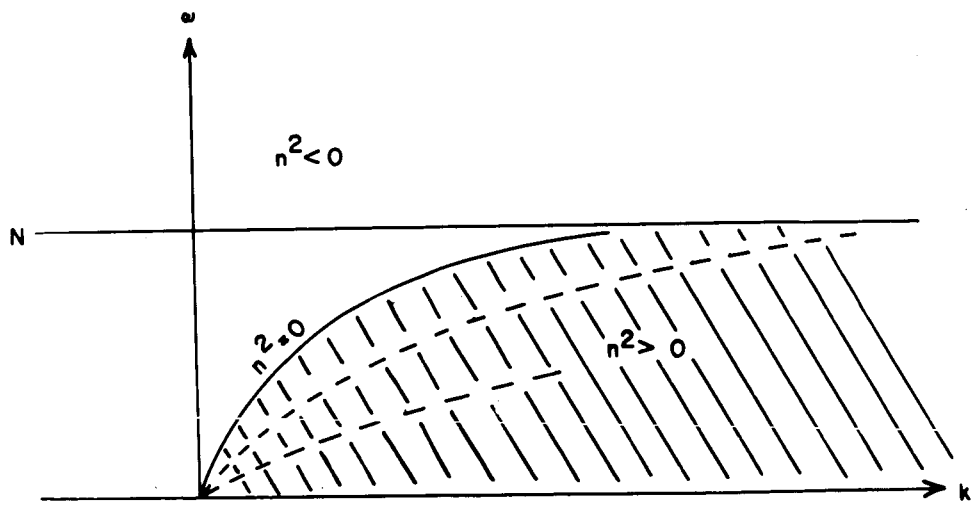

Fig. 2. Dispersion of plane internal waves in an infinite, incompressible fluid due to density stratification. (After Tolstoy, 1963)

Thus, "sound" waves of period > 5 minutes will not propagate.

4.4 Stratified, incompressible case with gravity. ($c = \infty$, $\nu \neq 0$, $g \neq 0$)

Again, using (4), (5) becomes

$$n^2 = k^2 \left[\frac{N^2}{\omega^2} - 1\right] - \nu^2$$

or

$$\omega_i = \frac{kN}{(k^2 + n^2 + \nu^2)^{1/2}} \tag{10}$$

where

$$N^2 = 2\nu g \tag{11}$$

We note immediately that we must have $N^2 > \omega^2$, i.e., N is a high frequency cut-off for propagating waves. Also, since k and n are no longer symmetric in the equations, propagation is anisotropic, as well as dispersive.

Graphing as before in Figure 2 (after Tolstoy, 1963) we see the cut-off and also that the largest group and phase velocities occur near $\omega = 0$ while V, $U \to 0$ as $\omega \to N$.

4.5 Compressible stratified fluid with gravity. ($c \neq \infty$, $\nu \neq 0$, $g \neq 0$)

Equation (5) becomes

$$n^2 = \frac{\omega^2}{c^2} - k^2 + k^2 \frac{N^2}{\omega^2} - \nu^2 \tag{12}$$

where

$$N^2 = 2\nu g - \frac{g^2}{c^2} \tag{13}$$

(For the values used previously, this leads to a period of about 7 minutes.)

Equation (12) may be written with the aid of (8) and (10),

$$\frac{\omega^4}{\omega_a^2} - \omega^2 + \omega_i^2 = 0$$

Acoustic and internal type solutions are both present, and may be written

$$\omega_A^2 = \omega_a^2 \left[1 - \left(\frac{\omega_i}{\omega_a}\right)^2 + \ldots\right.$$

$$\omega_I = \omega_i^2 \left[1 + \left(\frac{\omega_i}{\omega_a}\right)^2 + \ldots\right. \tag{14}$$

The effect of gravity on acoustic waves and of compressibility on internal waves is of order

$$\frac{\omega_i^2}{\omega_a^2} ,$$

which Tolstoy (1963), shows to be only .2 at its maximum. To compare these solutions, we must first compare

$$\omega_0 = \frac{\gamma g}{2c} \quad \text{and} \quad N = (\gamma - 1)^{1/2} \frac{g}{c} .$$

Since $\gamma \sim 1.4$ in the atmosphere, $\omega_0 > N$. The results are shown in Fig. 3 (after Tolstoy, 1963). We see that the effect of the gravity on the acoustic waves or compressibility on the internal gravity waves is to move the solutions slightly toward each other. Again propagation is anisotropic and dispersive. We have therefore 3 regions separated by curves of $n^2 = 0$, which delimit the acoustic type solutions, the internal gravity type solutions, and the region between where no propagating body waves exist in an infinite medium. The line marked Lamb type waves in the region $n^2 < 0$ will be discussed later.

4.6 Fluid Motions in Acoustic Gravity Waves.

Having explored the dispersion diagram, let us consider the nature of the fluid motions. We saw from 4.2 that for a propagating wave we have the quantity h given by a sinusoidal function of altitude. However, from 4.1, it is clear that

$$W = \rho^{-1/2} h = \rho_0^{-1/2} e^{\nu z} h \qquad (15)$$

is an exponentially growing function of altitude. This does not lead to kinetic energy divergence, since

$$KE_v = 1/2 \rho W^2 = \frac{1}{2} \rho_0 e^{-2\nu z} (\rho_0^{-1/2} e^{\nu z} h)^2 = \frac{h^2}{2} \qquad (16)$$

which is bounded.

$$\text{Now } W' = (in + \nu) W \qquad (17)$$

and 2.13 becomes

$$U = \frac{-c^2 kn + i k c^2 (\nu - g)}{k^2 c^2 - \omega^2} W \qquad (18)$$

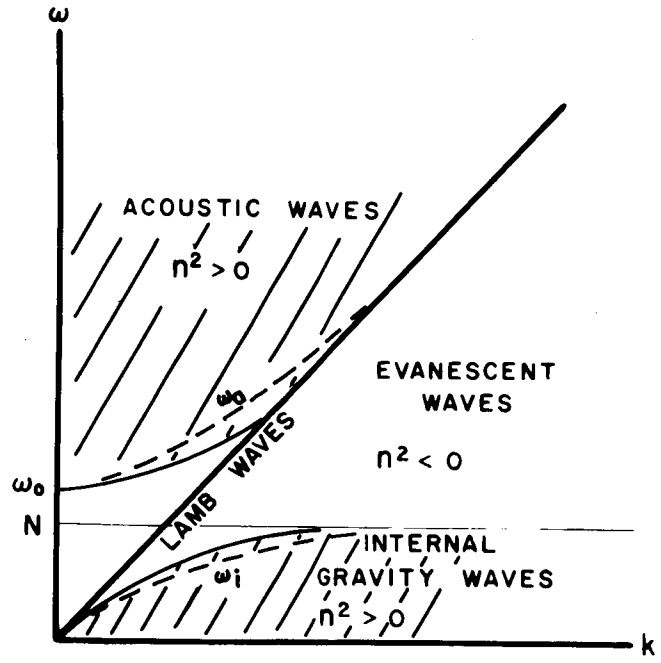

Fig. 3. Regions of solutions for a compressible, stratified fluid in a gravity field. Dashed curves correspond to neglect of gravity (ω_a) and compressibility (ω_i). (After Tolstoy, 1963)

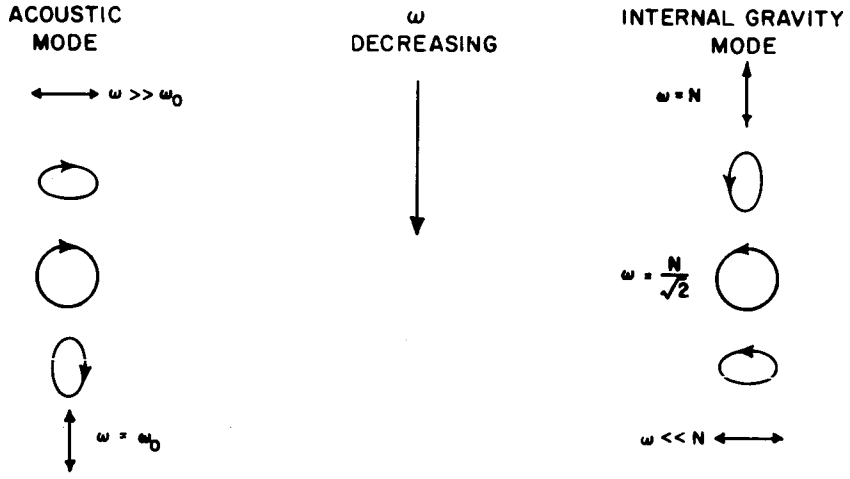

Fig. 4. Particle orbits for a horizontally propagating wave for the two families of solutions. The horizontal orbit size is much less than a wavelength.

Again, the horizontal kinetic energy density is obviously bounded.

We can derive the particle orbits from (18) without difficulty.

Acoustic Wave Orbits.

As noted above, gravity does not greatly affect the acoustic branch. For simplicity we shall set g = 0. Then, with (18) and introducing

$$u = \frac{\partial \xi}{\partial t} = i\,\omega\,\xi$$
$$w = \frac{\partial \zeta}{\partial t} = i\,\omega\,\zeta \qquad (19)$$

$$\xi = \frac{k\,(n - i\nu)}{n^2 + \nu^2}\,\zeta \qquad (20)$$

Putting

$$\zeta = \cos \omega t; \quad \xi = \frac{k\nu}{n^2 + \nu^2} \sin \omega t + \frac{kn}{n^2 + \nu^2} \cos \omega t \qquad (21)$$

and the particle orbit is given by

$$\xi^2 + \frac{k^2}{n^2 + \nu^2}\,\zeta^2 - \frac{2\,kn}{n^2 + \nu^2}\,\xi\zeta = \frac{k^2\,\nu^2}{(n^2 + \nu^2)}\,, \qquad (22)$$

the equation of an ellipse with tilted axes (for $n^2 + \nu^2 > 0$).

For high frequencies, $n^2 >> \nu^2$, (22) reduces to

$$\frac{\xi}{\zeta} = \frac{k}{n} \qquad (23)$$

indicating linear motion in the direction of propagation, as with standard acoustic waves. In the particular case of a horizontally propagating wave (n = 0), (22) becomes

$$\xi^2 + \frac{k^2}{\nu^2}\,\zeta^2 = \frac{k^2}{\nu^2}\,, \qquad (24)$$

indicating displacement transverse to the direction of propagation, tending toward being completely transverse as $k \to \infty$. It is easy to demonstrate that the vorticity = $\frac{\partial u}{\partial z} - \frac{\partial w}{\partial x}$ is not zero. Only in fluids of uniform density are sound waves purely longitudinal and irrotational. From (21) it can be seen that the particle traces its orbit in a clockwise direction.

Gravity Waves.

We may start with 2.13, set $c = \infty$, and make use of (19) to find

$$\xi = -\frac{n + i\nu}{k}\zeta \tag{25}$$

and again if

$$\zeta = \cos \omega t$$

$$\xi = -\frac{\nu}{k}\sin \omega t - \frac{n}{k}\cos \omega t$$

then

$$\xi^2 + \zeta^2\left(\frac{N^2}{\omega^2} - 1\right) + 2\frac{n}{k}\xi\zeta = \frac{\nu^2}{k^2} \tag{26}$$

which is also the equation of a tilted ellipse for $\omega < N$.

Again looking only at horizontal propagation, for $\omega \sim N$,

$$k = \left[\frac{n^2 + \nu^2}{N^2/\omega^2 - 1}\right]^{1/2} \to \infty , \qquad \xi \to 0 \tag{27}$$

and the motion is transverse. As $\omega \to 0$

$$\zeta \to 0 \tag{28}$$

$\xi \to \nu/k$, and the motion is again longitudinal. This behavior and the intermediate steps are summarized in Fig. 4. From (26) the trajectory is executed in a counterclockwise direction - opposite to acoustic waves.

Midgley and Liemohn (1966) have given a very interesting discussion of particle orbits and propagation.

4.7 Polarization Relationships.

Taking the form from 1, we can write

$$W/Z = U/X = \frac{P_1}{p_0 P} = \frac{\rho_1}{\rho_0 R} \propto A\,\rho^{-1/2}\, e^{i(kx + nz - \omega t)}$$
$$\propto A\, e^{\nu z}\, e^{i(kx + nz - \omega t)} \tag{20}$$

where A is a constant, presumed small.

Substitution in equations 2.1, 2.4, and 2.13 leads to the following polarization relations:

$$
\begin{aligned}
Z &= \omega(\omega^2 - k^2 c^2) \\
X &= \omega k c^2 [n + i g/c^2 (1 - \gamma/2)] \\
P &= \gamma\omega^2 [n + i g/c^2 (1 - \gamma/2)] \\
R &= n\omega^2 - i k^2 g (\gamma - 1) + i \frac{\gamma g \omega^2}{2c^2}
\end{aligned}
\tag{30}
$$

These relationships may be thought of as representing vectors on a complex diagram, showing the relative amplitudes and phases of the different oscillating components.

Note that these relationships indicate the percentage perturbation of pressure and density increases with height. A height will be reached where our perturbation treatment will not be applicable, and non-linear effects must be considered.

At very low frequencies, we have

$$R/X \simeq \frac{i (\gamma - 1)^{1/2}}{c} \tag{31}$$

which relates density perturbations to horizontal velocities.

We can crudely think of the motions in the following qualitative ways. For the acoustic waves, fluid comes together, is compressed, and sinks into a denser region before the compressed fluid elastically expands and is buoyed up on the second half of the cycle.

For gravity waves, fluid comes together too slowly to be greatly compressed. It sinks, is compressionally heated; its density becomes lower than its surroundings and it is buoyed back up, causing the fluid flow direction to reverse.

Midgley and Liemohn (1966) have discussed the physical details much more carefully.

5. Phase and Group Velocities; Propagation Surfaces and Energy Flow

The information of Section 4.5 can be seen in another way. By picking an ω, as a period ($= \frac{2\pi}{\omega}$), for a series of k we may solve for n. The points k, n for a given ω are plotted in Figure 5, taken from Hines (1960). Such surfaces are known as propagation surfaces, and are discussed also by Tolstoy (1963) and Eckart (1960). The family of ellipses represents a sequence of acoustic waves, while the hyporbolas represent internal gravity waves.

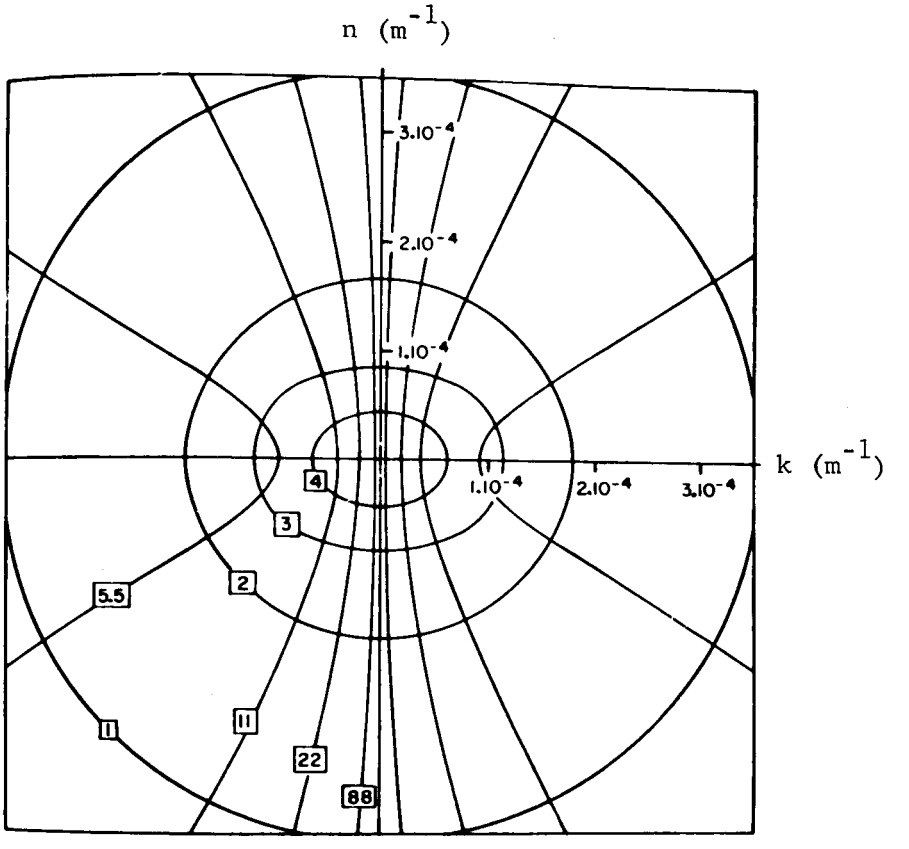

Fig. 5. Propagation surfaces of acoustic gravity waves. The periods in minutes are shown in boxes on the corresponding curves. The cut off periods for acoustic and gravity waves are 4.4 and 4.9 minutes respectively. (After Hines, 1960)

An interesting point can also be noted here. Looking at the hyperbola for a particular period, we see that the ratio k/n is nearly constant over all but a small part of the curve. For waves of that period, with horizontal wavelengths somewhat less than the maximum, the wave can only propagate in one direction; alternatively, the frequency depends only on the direction of propagation. This point is also noted by Landau and Lifshitz (1959, pp. 44-46). The longer periods propagate closer to the vertical, but note that these waves cannot propagate vertically. For long period gravity waves, then, we have a family of wave fronts tilted slightly from the horizontal, moving upward or downward.

Remembering that $V_x = \frac{\omega}{k}$; $V_z = \frac{\omega}{n}$, we can form a refractive index vector $\eta_x = \frac{ck}{\omega}$, $\eta_z = \frac{cn}{\omega}$.

This is plotted in the next figure (6) (after Hines, 1960). Here the distance from the origin gives the index of refraction - waves with period less than 1 minute are seen to propagate isotropically with the speed of sound, while smaller η values represent more rapid propagation. Note that acoustic wave phase may propagate much more rapidly near ω_0 than in the high frequency limit, and more rapidly vertically. Internal gravity wave phase propagates more slowly than sound, and more rapidly horizontally.

The group velocity may be written

$$U_x = \frac{\partial \omega}{\partial k}, \qquad U_z = \frac{\partial \omega}{\partial n}$$

and is known from general considerations to be the velocity of energy propagation. Since the lines in the last figure are lines of constant ω, we see that U is perpendicular to these lines and directed toward shorter periods. This is illustrated in the inset, where it is clear that the vertical direction of energy propagation may be opposite to the direction of phase propagation. Specifically, a downward phase propagation may accompany upward energy propagation, although for longer periods the flow is nearly horizontal. See also Eckart (1960).

6. Boundary Conditions and Boundary Waves

At a rigid horizontal surface, the normal velocity must vanish, or

$$W = 0 \qquad (1)$$

At the surface between two compressible fluids (labeled 1 and 2) of different densities, we require

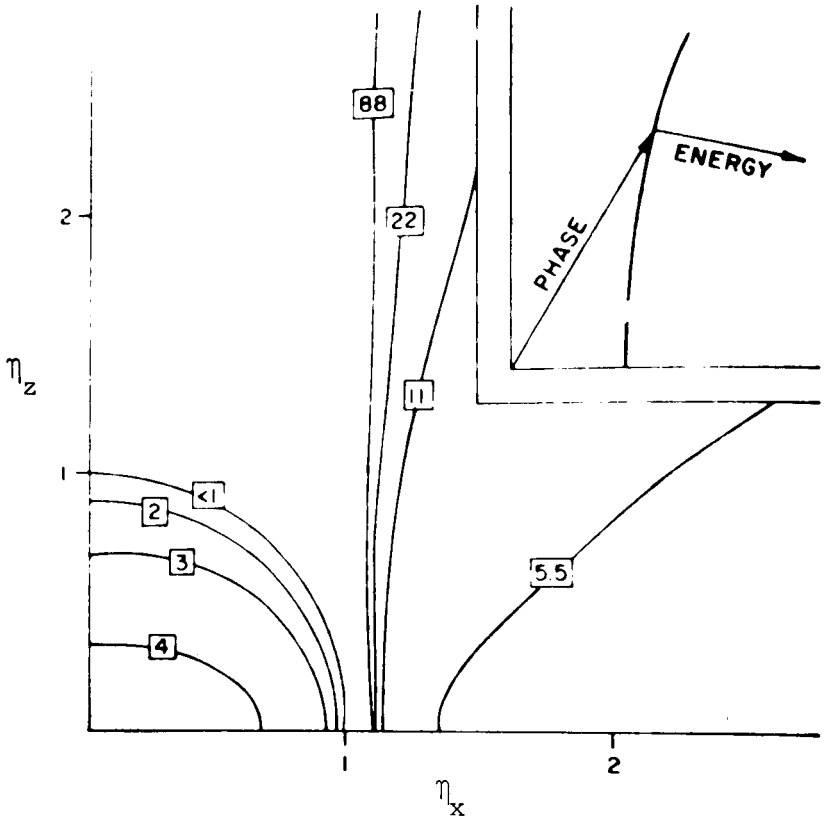

Fig. 6. Contours of constant period in the η_x, η_z domain. The periods (in minutes) are shown in boxes on the corresponding curves. The basic parameters are as for Fig. 5. The relation between phase and energy progression is indicated by the geometric construction in the inset. (After Hines, 1960)

$$W_1 = W_2 \tag{2}$$

and

$$p_1 = p_2 \tag{3}$$

However, since the surface separating the fluids also moves, we must express this as

$$\frac{Dp_1}{Dt} = \frac{Dp_2}{Dt} \tag{4}$$

Since

$$\frac{Dp}{Dt} = c^2 \frac{D\rho}{Dt} = - c^2 \rho \nabla \cdot \vec{v} \tag{5}$$

condition (5) may be written (for our 2-dimensional case)

$$c_1^2 \rho_1 [i k U_1 + W_1'] = c_2^2 \rho_2 [i k U_2 + W_2'] \tag{6}$$

For the case of a free surface, $\rho_2 = 0$, and (6) becomes

$$i k U_1 + W_1' = 0 \tag{7}$$

In general, remembering

$$U = i k \frac{c^2 W' - g W}{k^2 c^2 - \omega^2}$$

we have

$$\rho_1 (k^2 g W_1 - \omega^2 W_1') = \rho_2 (k^2 g W_2 - \omega^2 W_2') \frac{c_2^2 (k^2 c_1^2 - \omega^2)}{c_1^2 (k^2 c_2^2 - \omega^2)} \tag{8}$$

Boundary Waves

The presence of boundaries allows additional wave types to those discussed above. Boundary waves are waves whose energy is concentrated at a boundary of discontinuity of one or more parameters (c, ρ, ρ') and correspond to $n^2 < 0$ on both sides of the boundary - i.e., an exponential variation of amplitude. On physical grounds, we demand that these waves give a vanishing of energy density as $z \to \infty$.

Tolstoy (1963) discusses these waves for several situations. We will mention only two which are of particular interest.

The first of these is the Lamb wave (Lamb, 1945, p. 548). Here we satisfy B. C. (1) by setting $W \equiv 0$ everywhere. Then, from 2.12,

$$\not{i}\,\not{k}\, g\, \rho\, U + \frac{\partial}{\partial z}\left(\rho\, c^2\, \not{i}\,\not{k}\, U\right) = 0 \tag{9}$$

$$\frac{g}{c^2}\left(\rho\, c^2\, U\right) + \frac{\partial}{\partial z}\left(\rho\, c^2\, U\right) = 0 \tag{10}$$

$$\rho\, c^2\, U = \left(\rho\, c^2\, U\right)_{z=0}\, e^{-g/c^2 z}, \qquad z > 0 \tag{11}$$

or

$$U = U_{z=0}\, e^{(2\nu - g/c^2)z} \qquad z > 0 \tag{12}$$

if c^2 = constant.

Stability of the medium requires $2\nu > g/c^2$, so the amplitude increases with height. However,

$$\rho\, U^2 \propto e^{-2\nu z}\, e^{2(2\nu - g/c^2)z} = e^{2(\nu - g/c^2)z} \tag{13}$$

which does go to zero.

Another wave in a stratified compressible fluid, at a free surface of medium 2, $z < 0$, is found from (8), with $\rho_1 = 0$.

$$k^2 g\, W_2 - \omega^2\, W_2' = 0 \tag{14}$$

We are looking for solutions of the form

$$W_2 \propto e^{-\nu_2 z}\, e^{n_2' z} \tag{15}$$

Then we have as a dispersion relation

$$\frac{k^2 g}{\omega^2} = \nu_2 + n_2' \tag{16}$$

where

$$n_2' = i\, n_2 = \left[k^2 - \frac{\omega^2}{c^2} - \frac{k^2}{\omega^2}\, \mathbb{N}^2 + \nu_2^2\right]^{1/2} \tag{17}$$

is real.

This has surface waves, and also, substituting

$$\omega = kc \tag{18}$$

into (17) one finds

$$n_2' = \left(\frac{g}{c^2} - \nu_2\right) \tag{19}$$

Putting (19) and (18) into (16) proves that (18) is a solution. By (15), we have

$$W_2 \propto e^{(g/c^2)z} \qquad z < 0$$

This represents a horizontally traveling sound wave, with a small vertical component arising from buoyancy effects in the gravity field. The condition for energy density → 0 as $z \to -\infty$ is the same as for the Lamb wave. These we may term Lamb-type waves.

We can make the following remarks about the Lamb waves and Lamb-type waves. First, they are not true boundary waves, but modified acoustic waves, traveling parallel to the density stratification. Second, they need the presence of a boundary, to prevent the local energy density from becoming infinite in one direction.

The position of these waves has previously been indicated on the diagnostic diagram.

7. Reflection and Transmission Coefficients.

7.1 Some general remarks.

The standard procedure for obtaining reflection and transmission coefficients at an interface between layers with constant coefficients is to consider a wave of unit amplitude incident on a boundary, which is partly reflected (with amplitude R) and partly transmitted with amplitude T. The boundary conditions are invoked to solve for R and T. If the incident wave is in medium, 1, these are respectively

$$e^{i(kx+n_1 z-\omega t)}$$

$$R\, e^{i(kx-n_1 z-\omega t)}$$

$$T\, e^{i(kx+n_2 z-\omega t)}$$

It is interesting to note that this only specifies the ω, k of the transmitted wave. If the two media are somewhat different, so that the $\omega(k)$ acoustic curves of the first medium intersect the internal wave

solutions of the second medium, we have sufficient conditions to allow transformation of an acoustic wave to an internal wave. As we saw before, this will be possible if $c_2 > c_1$. An obvious condition is that

$$N_2 > \nu_1 c_1 = \omega_1.$$

It is also necessary that the slope of the internal wave solution for 2 near $\omega = 0$ exceed c_1. These are not sufficient, since they do not require the intersection of ω_1 and ω_2 curves.

7.2 Calculation of the Reflection Coefficient.

We will illustrate the technique by considering discontinuities in density gradient in the presence of a gravity field. We have two half spaces in contact at $z = 0$.

In half space 1, $z < 0$ $\qquad \rho_1 = \rho_0 e^{-2\nu_1 z}$

while in half space 2, $z > 0$ $\qquad \rho_2 = \rho_0 e^{-2\nu_2 z}$

while $\qquad c_1 = c_2$

Now $W_1 = \rho_1^{-1/2} h_1 = \rho_1^{-1/2} \left(e^{i(kx+n_1 z-\omega t)} + R\, e^{i(kx-n_1 z-\omega t)} \right)$

$$W_2 = \rho_2^{-1/2} h_2 = \rho_2^{-1/2} T\, e^{i(kx+n_2 z-\omega t)}$$

Applying the boundary conditions 6.2 and 6.8, at $z = 0$ leads immediately to

$$1 + R = T$$

$$\nu_1 (1 + R) + i\, n_1 (R - 1) = (\nu_2 - i\, n_2)\, T$$

from whence

$$R = \frac{\nu_2 - \nu_1 + i\,(n_1 - n_2)}{\nu_1 - \nu_2 + i\,(n_1 + n_2)}$$

If n_2 is imaginary and n_1 real,

$$n_2 = i\, n_2'$$

and $R = e^{-2i\chi}$

where $\chi = \tan^{-1} \frac{\nu_2 - \nu_1 + n_2'}{n_1}$

since $|R| = 1$, this corresponds to total reflection of plane body waves. Recalling

$$n^2 = \frac{\omega^2}{c^2} - k^2 + \frac{k^2 N^2}{\omega^2} - \nu^2$$

$$N^2 = 2\nu g - g^2/c^2$$

we see that if $\nu_1 < \nu_2$, then $N_1 < N_2$, and only acoustic waves will be reflected. On the other hand, if $\nu_2 < \nu_1$, $N_2 < N_1$, then only internal gravity waves would be subject to total reflection.

These results are shown graphically in Fig. 7, for $\nu_1 < \nu_2$.

Looking at Fig 7(a) it is clear that gravity waves in the lined area (in region 2) will not propagate in region 1, while acoustic waves in the cross hatched area (in region 1) will not propagate in region 2. This indicates that these waves will be reflected, as shown in (b). In this case we have total reflection of energy from the interface with a change of phase given by 2χ.

If we have a 3 layer structure, with a region 2 of finite thickness between two semi-infinite spaces of region one, we would expect that internal gravity wave energy once in the layer, would propagate along it, unable to get out. See Fig. 8.

This occurs because region 2 is a region of large N. In the atmosphere, we expect regions of maximum N to act as channels for internal waves.

Similarly, a region of minimum ω_0 acts as a trap for acoustic waves, as does the classical low sound velocity channel.

These processes are counterparts of the optical processes of total internal reflection, and the layers mentioned above are similar to "light pipes".

8. Reflection and Duction in the Atmosphere.

With the general ideas of reflection, let us explore some possible cases. We note first that for an isothermal layer

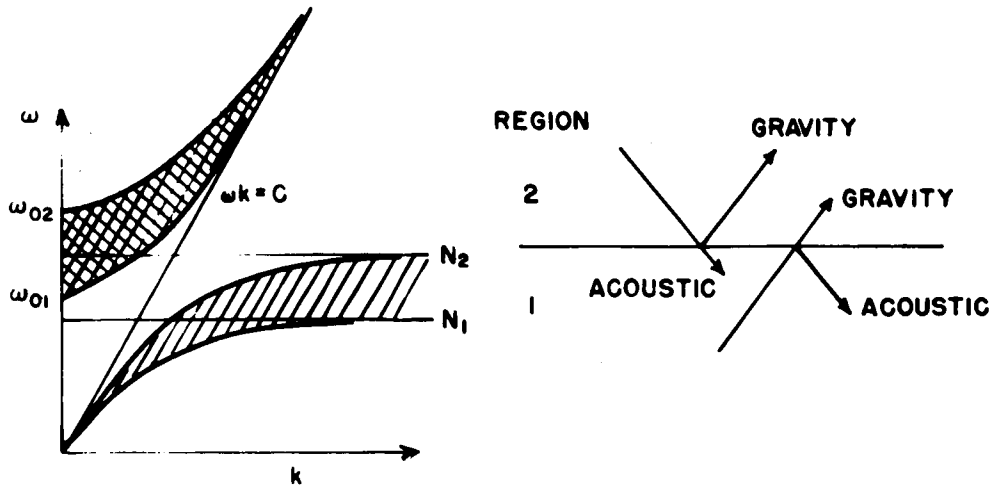

Fig. 7. Differences of characteristic diagrams for two half-spaces when $\nu_1 < \nu_2$ and resulting reflections.

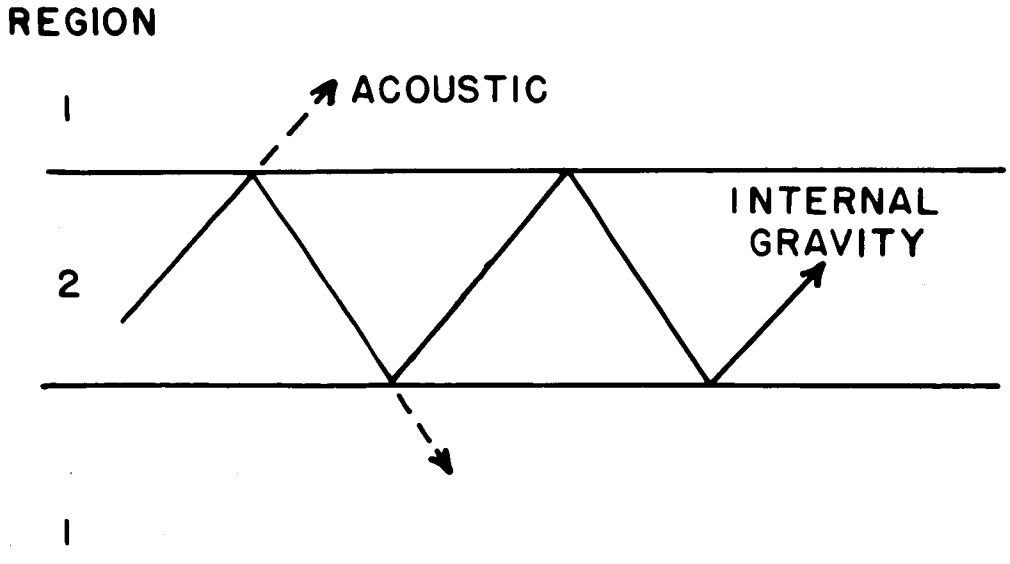

Fig. 8. Schematic indication for ducting by a region of large N.

$c \propto T^{1/2}$; $\nu \propto 1/T$; $\omega_0 \propto c\nu \propto T^{-1/2}$; $N^2 \propto T^{-1}$; $N \propto T^{-1/2}$.

Thus, for a warm layer 1, cold layer 2, we may draw the diagram (see Fig. 9) for waves incident from region 1.

In this case, sound waves below a certain frequency will be reflected by the cold layer, as will some of the gravity waves with $n_1 \approx 0$. However, those with $n_1 >> 0$ (propagating upward more strongly) will enter region 2.

In this case, the warm layer acts to reflect high frequency sound waves and internal waves, while letting low frequencies pass through. Note that this latter is due to a region of large N values in the region of incidence, while the former is due to the higher sound velocity in region 2.

In Figure 11, from Tolstoy (1963), we see a plot of c, N, and ω_0 for the atmosphere for the lowest 200 km. Looking at the curve for c (which is $T^{1/2}$) we see that very broadly we can categorize the atmosphere by a succession of regions with warm troposphere, cold stratosphere, warm stratopause region, colder mesopause, and hot thermosphere. Thus qualitatively we could expect a series of reflecting layers, reflecting different types of waves, with the warm thermosphere being the most important. However, when we consider layers rather than half-spaces, we must ask whether the slab is thick enough to act as a half space. Physical insight, from quantum mechnics and optics suggest that an incident wave may penetrate about one wavelength into a region where it has an imaginary wave number. If the thickness of the layer or layers is greater than this, we may expect our half-space insight to hold. If the layer is appreciably less thick than this, the wavelength will not notice this region very much, and integrate its effect with that of the regions of real wave number on either side.

We note also that regions of ducting are clearly shown:

1) Min ω_0 - most important in thermosphere
2) Max N - Upper mesosphere, stratosphere
3) Min c - Upper mesosphere, stratosphere.

Again, wavelength considerations must be borne in mind - too long a wavelength may not be trapped, and also may not "fit" in the waveguide.

A final point should be made here. In a non-isothermal atmosphere,

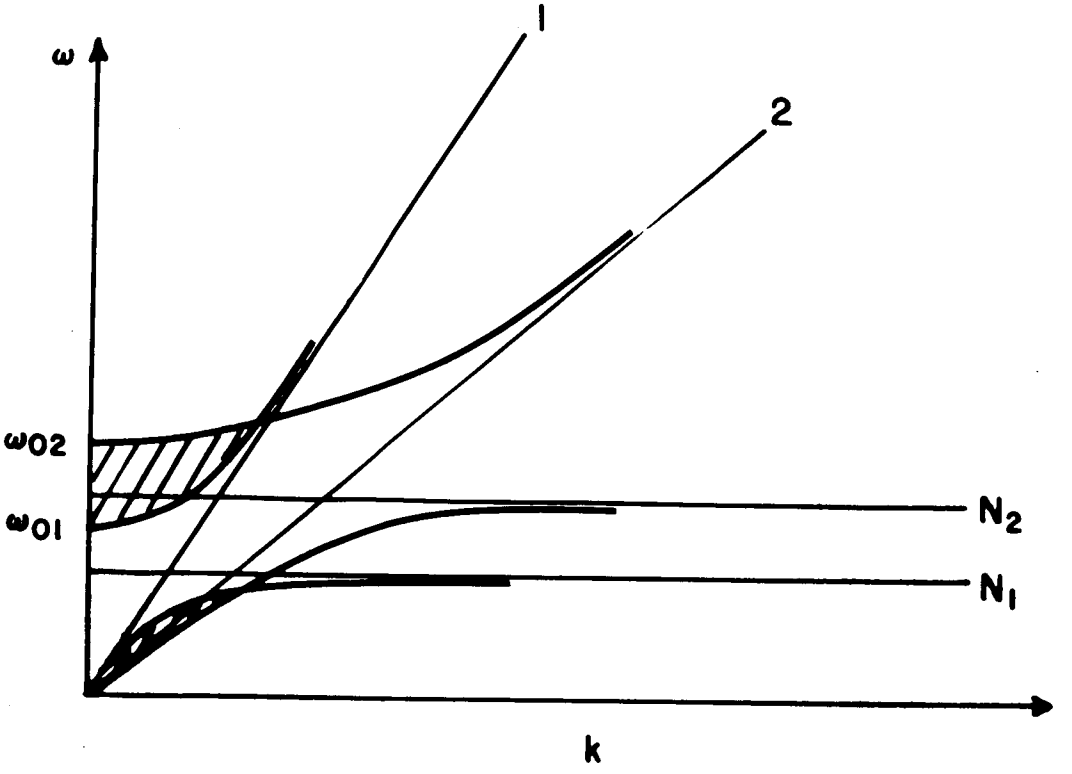

Fig. 9. Differences of characteristic diagrams for warm half-space 1, cold half-space 2. Shaded areas show reflection by region 2.

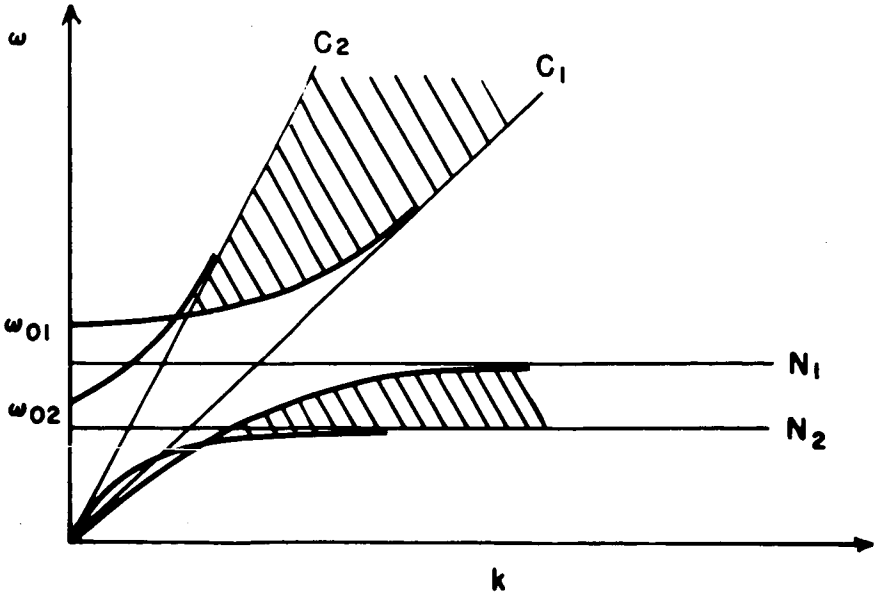

Fig. 10. Differences of characteristic diagrams for cold half-space 1, warm half-space 2. Shaded areas show reflection by region 2.

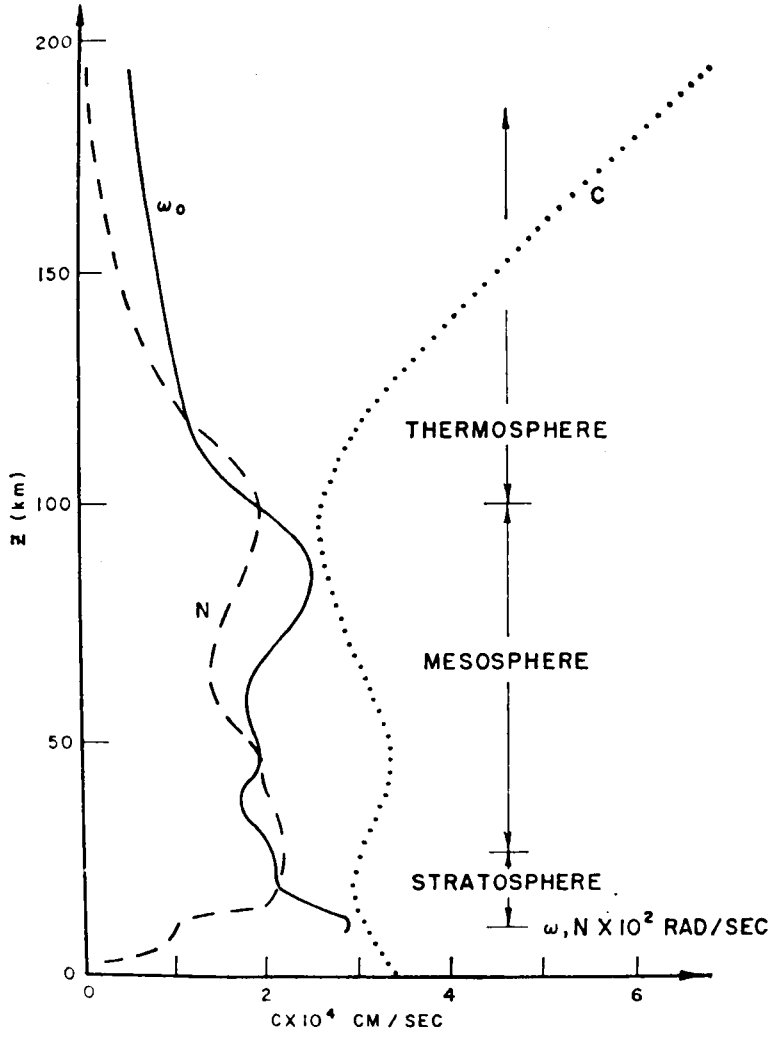

Fig. 11. Structure of the earth's atmosphere. (After Tolstoy, 1963)

$1/\rho \frac{d\rho}{dz}$ can be large, and $N > \omega_0$. This is shown for two regions of the atmosphere in Figure 11, where dT/dz exceeds about 2.3°/km. In this case, the gravity and acoustic wave sequences can not be separated. The plot in refractive index space with ω as parameter is shown in Figure 12 (taken from Hines, 1960). The change is not great for $\omega < .3\omega_0$ or $\omega > 3N$, but when $\omega_0 < \omega < N$ there is a complete change in the diagram. An internal gravity wave with large horizontal and vertical wavelength may propagate much faster than the speed of sound, while sound waves may propagate more slowly. Most distressing, the direction of energy propagation can reverse in a very narrow interval, passing through infinite values.

In the next lecture, we shall consider the propagation of waves in a realistic atmosphere.

Acknowledgements.

The support of NASA Grant NSG-173 and the Florida State University in the preparation of this review is gratefully acknowledged. I thank Professors Seymour L. Hess and Richard L. Pfeffer for their encouragement.

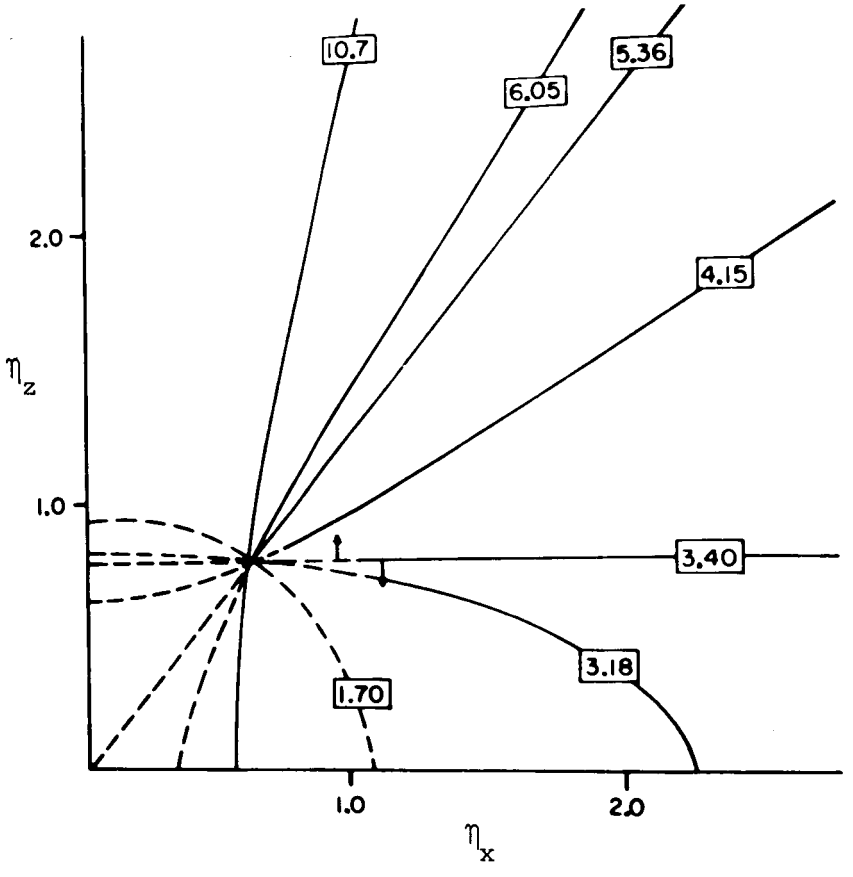

Fig. 12. Contours of constant period in the η_x - η_z domain, for a region where the acoustic cut off period is 5.36 min., and the gravity wave cut off is 3.40 min. (After Hines, 1960)

References

Eckart, C., 1960: Hydrodynamics of Oceans and Atmospheres. New York, Pergamon Press, 284 pp.

Eliassen, A. and E. Kleinschmidt, 1957: Handbuch der Physik, 48. Berlin, Springer Verlag, pp. 1-154.

Heines, C. O., 1960: Internal atmospheric gravity waves at ionospheric heights. Can. J. Phys., 38, 1441-1481.

Lamb, H., 1945: Hydrodynamics. New York, Dover Publications, 738 pp.

Landau, L. D. and E. M. Lifshitz, 1959: Fluid Mechanics (English Translation), London, Pergamon Press, pp. 44-46.

Midgley, J. E. and H. B. Liemohn, 1966: Gravity Waves in a realistic Atmosphere. J. Geoph. Res., 71, 3729-3748.

Tolstoy, J., 1963: The theory of waves in stratified fluids including the effects of gravity and rotation. Revs. Mod. Phys., 35, 207-230.

Acoustic-Gravity Wave Ducting in the Atmosphere by Vertical Temperature Structure

Acoustic-Gravity Wave Ducting in the Atmosphere by Vertical Temperature Structure

1. Early Studies of Atmospheric Wave Propagation

Lamb (1945) and Pekeris (1948) considered the propagation of waves in one layer atmospheres, with both uniform temperatures and constant lapse rates. Pekeris (1948) and Scorer (1950) also considered analytically the propagation in an atmosphere with a troposphere having a constant lapse rate and an isothermal stratosphere. They both found solutions involving confluent hypergeometric functions, and it is clear that an attempt to extend this to many layers would be an involved project.

In addition, both predicted the existence of a cut off frequency, below which waves would not propagate. This may be understood by considering the temperature distribution used by Pekeris (Fig. 1). This may be approximated by a two layer atmosphere, with the lower layer warmer, as shown in Figure 2.

The shading represents the regions where propagating stratospheric solutions exist; tropospheric waves in these parts of the diagram will continue on upward, and be absent at the suface far from the source. Conversely, those solutions for the troposphere which cannot propagate in the stratosphere are reflected, channeled in the troposphere, and observable at great distances. Above ω_c we see that no trapping exists, and thus high frequency (short period) waves should be absent from barograms of nuclear explosions measured several thousand kilometers from the detonation, if the atmosphere has such a structure.

In fact, the solution Pekeris found corresponds to the Lamb type waves, but again the same reasoning holds - those trapped will be seen at large distance, those not trapped will "leak" upward and no appreciable energy will remain at the surface at great distances.

The observations of these short-period waves led Yamamoto (1957) and Hunt, Palmer and Penney (1960) to consider more complex atmospheres. Rather than consider their results explicitly, let us see how the problem was formulated by Pfeffer (1962) and Press and Harkrider (1962) and see the results for some simple but illustrative atmospheres calculated by Pfeffer and Zarichny (1962).

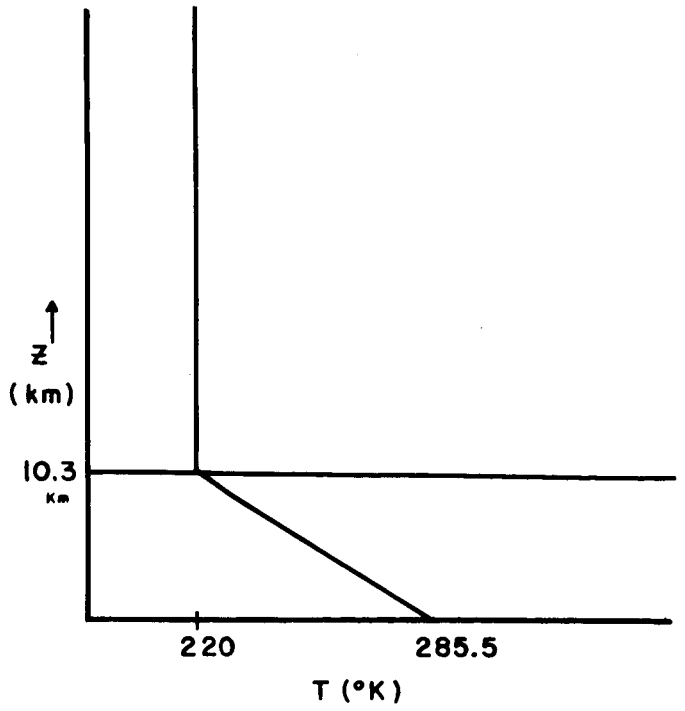

Fig. 1. Temperature distribution considered by Pekeris.

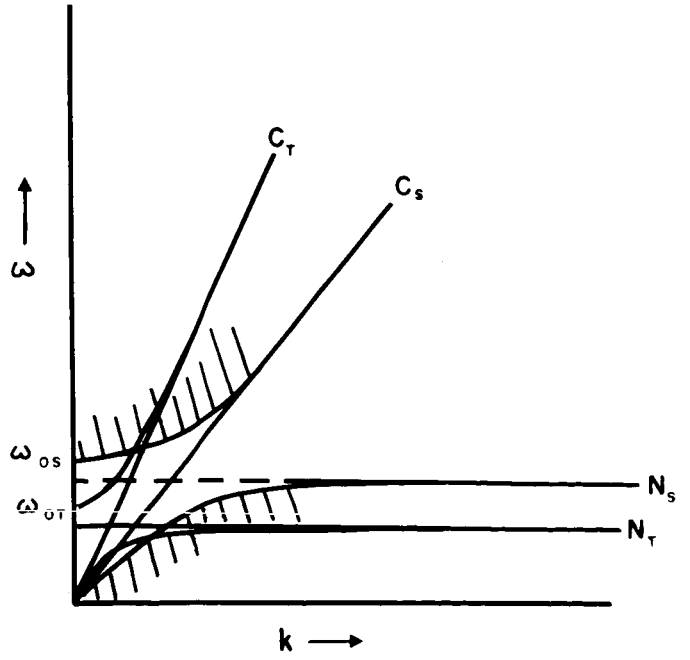

Fig. 2. Characteristic diagram for two layer atmosphere with warm troposphere, cold stratosphere.

2. Matrix Formulation of the Isothermal Layer Approach.

We shall discuss the formulation due to Pfeffer (1962), (hereafter referred to as P). That of Press and Harkrider (1962) (PH) is very similar. Both of these papers treated the calculation of the disturbance at a large distance from a point explosive source, and so used cylindrical geometry. This is not necessary in a general consideration of free modes; we shall continue to use rectangular coordinates.

The method is to write a soluble equation for one quantity, write a general form of the solution in each layer with undetermined coefficients, then determine the coefficients from the boundary conditions on pressure and vertical velocity. Following the classical treatments, we may write an equation for the divergence, defined as

$$d = \frac{\partial u}{\partial x} + \frac{\partial w}{\partial z} .$$

We assume

$$d = D(z)\, e^{i(kx-\omega t)} , \qquad p_1 = P(z)\, e^{i(kx-\omega t)}$$

Then, remembering equations 2.11, 2.12, and 2.10 from the first lecture,

$$\rho \frac{\partial^2 u}{\partial t^2} = - g\rho \frac{\partial w}{\partial x} + \frac{\partial}{\partial x}\left[\rho c^2 \left(\frac{\partial u}{\partial x} + \frac{\partial w}{\partial z}\right)\right] \qquad A$$

$$\rho \frac{\partial^2 w}{\partial t^2} = g\rho \frac{\partial u}{\partial x} + \frac{\partial}{\partial z}\left|\rho c^2 \left(\frac{\partial u}{\partial x} + \frac{\partial w}{\partial z}\right)\right| \qquad B$$

$$\frac{\partial p_1}{\partial t} = wg\rho - \rho c^2 \left(\frac{\partial u}{\partial x} + \frac{\partial w}{\partial z}\right) \qquad C$$

we obtain, by taking $\frac{\partial}{\partial x}$ of A + $\frac{\partial}{\partial z}$ of B

$$D'' + \left(\frac{dc^2}{dz} - g\gamma\right)\frac{1}{c^2} D' + \left[- k^2 + \frac{\omega^2}{c^2} + \frac{k^2}{\omega^2}\left(\frac{g}{c^2}\frac{dc^2}{dz} + N^2\right)\right] D = 0 \qquad (1)$$

Taking $\frac{\partial^2}{\partial t^2}$ of B and substituting from A

$$(g^2 k^2 - \omega^4)\, W = \omega^2 c^2 D' + g\,(c^2 k^2 - g\,\omega^2)\, D \qquad (2)$$

and from C

$$P = \frac{i\rho}{\omega}\,(c^2 D - g\, W) \qquad (3)$$

(see also Lamb, 1945).

Equation (1) is a second order differential equation with variable coefficients - the one used by Pekeris (1948) which has confluent hypergeometric functions as its solutions. Instead of trying to extend this treatment, P assumed that each layer was isothermal (i.e., c^2 = constant) and used a large number of layers to express the temperature variation.

For the n^{th} layer, we have

$$D'' - \frac{g\,\gamma}{c_n^2} D' + \left[- k^2 + \frac{\omega^2}{c_n^2} + \frac{k^2}{\omega^2} N_n^2 \right] D = 0 .$$

Solutions may be expressed as

$$D(z) = e^{\nu_n z} \left[a_n e^{n'_n z} + b_n e^{-n'_n z} \right] \qquad (4)$$

where z is measured from the base of the layer, and

$$n' = in = -i \left[\frac{\omega^2}{c^2} - k^2 + \frac{k^2}{\omega^2} N^2 - \nu^2 \right]$$

Putting (4) into (2) gives

$$\begin{aligned} [g^2 k^2 - \omega^4]\, W = {} & a_n \left[g\, c_n^2 k^2 - \tfrac{1}{2} g\gamma\, \omega^2 + \omega^2 c_n^2 n'_n \right] e^{\nu_n z} e^{n'_n z} \\ & + b_n \left[g\, c_n^2 k^2 - \tfrac{1}{2} g\, \gamma\, \omega^2 - \omega^2 c_n^2 n'_n \right] e^{\nu_n z} e^{-n'_n z} \end{aligned} \qquad (5)$$

Putting (4) and (5) into (3) results in

$$\begin{aligned} -\frac{i}{\rho_n \omega} \left[g^2 k^2 - \omega^4 \right] P = {} & a_n \left[\tfrac{1}{2} g^2 \gamma - \omega^2 c_n^2 - g\, c_n^2 n'_n \right] e^{\nu_n z} e^{n'_n z} \\ & + b_n \left[\tfrac{1}{2} g^2 \gamma - \omega^2 c_n^2 + g\, c_n^2 n'_n \right] e^{\nu_n z} e^{-n'_n z} \end{aligned} \qquad (6)$$

Now P and W are expressed in terms of the a's and b's. We could have begun by writing a general form of the solution for W, then expressing P in terms of this, and applying the boundary conditions. This results in a slightly more cumbersome set of equations (Pfeffer, private communication) although the results would be equivalent.

To eliminate the 2N constants, we must apply 2N boundary conditions. These are

1. At the surface, $W = 0$.
2. In the top layer (a half-space) the total kinetic energy is finite; i.e., $a_N = 0$. Also, Pfeffer required that n'_N be real, since the interest was in propagating, not attenuating waves.

At each of the N - 1 interfaces between layers, we require

1. Vertical velocities on both sides of the interface to be equal.
2. The total pressure be continuous across the interface; put in the form $p_m(z) - g\,\rho_{Cm}\,\zeta = p_{m+1}(z) - g\,\rho_{Cm+1}\,\zeta$

where ζ is the height of the interface above its equilibrium value, and p_m is the perturbation pressure in the m^{th} layer.

Since

$$\frac{\partial \zeta}{\partial t} = i\,\omega\,\zeta = w$$

these boundary conditions can be formulated

$$\begin{bmatrix} W_B \\ P_B \end{bmatrix}_{n+1} = \begin{bmatrix} 1 & 0 \\ \frac{ig\Delta\rho_n}{\omega} & 1 \end{bmatrix} \begin{bmatrix} W_H \\ P_H \end{bmatrix}_n = \begin{bmatrix} F_n \end{bmatrix} \begin{bmatrix} W_H \\ P_H \end{bmatrix}_n \tag{7}$$

where B, H denote the bottom and top of the layers, and

$$\Delta\rho_n = \rho_{H,n} - \rho_{B,n+1}.$$

We can now write

$$\begin{bmatrix} W_H \\ P_H \end{bmatrix}_n = \begin{bmatrix} H_n \end{bmatrix} \begin{bmatrix} a \\ b \end{bmatrix}_n$$

$$\begin{bmatrix} W_B \\ P_B \end{bmatrix}_n = \begin{bmatrix} B_n \end{bmatrix} \begin{bmatrix} a \\ b \end{bmatrix}_n .$$

Then

$$\begin{bmatrix} W_H \\ P_H \end{bmatrix}_n = \begin{bmatrix} H_n \end{bmatrix} \begin{bmatrix} B_n \end{bmatrix}^{-1} \begin{bmatrix} W_B \\ P_B \end{bmatrix}_n$$

and from (7)

$$\begin{bmatrix} W_B \\ P_B \end{bmatrix}_{n+1} = \begin{bmatrix} F_n \end{bmatrix}\begin{bmatrix} H_n \end{bmatrix}\begin{bmatrix} B_n \end{bmatrix}^{-1} \begin{bmatrix} W_B \\ P_B \end{bmatrix}_n = \begin{bmatrix} M_n \end{bmatrix} \begin{bmatrix} W_B \\ P_B \end{bmatrix}_n .$$

By induction we write

$$\begin{bmatrix} W_B \\ P_B \end{bmatrix}_N = \Pi_{N-1} \begin{bmatrix} M_N \end{bmatrix} \begin{bmatrix} W_B \\ P_B \end{bmatrix}_1$$

or

$$\begin{bmatrix} W_{BN} \\ P_{BN} \end{bmatrix} = \begin{bmatrix} \theta_1 & \theta_2 \\ \theta_3 & \theta_4 \end{bmatrix} \begin{bmatrix} 0 \\ P_{B1} \end{bmatrix} \tag{8}$$

which may be written

$$\theta_4 W_{BN} - \theta_2 P_{BN} = 0, \tag{9}$$

where

$$W_{BN} = \frac{g c_N^2 k^2 - \frac{g \gamma \omega^2}{2} - \omega^2 c_N^2 n'_N}{g^2 k^2 - \omega^4} b_N$$

$$P_{BN} = \frac{\rho\, i\, \omega \left[\frac{1}{2} g^2 \gamma - \omega^2 c_N^2 + g\, c_N^2\, n_N'\right]}{g^2 k^2 - \omega^4} b_N$$

This is the dispersion relationship. By specifying c^2 and thickness of each layer, we can solve for $\omega(k)$ or $V = \omega/k$ or $U = \frac{d\omega}{dk}$. In practice, this is done by a trial and error method, in the following manner:

(1) select k;

(2) guess an ω as a solution;

(3) evaluate the $[M_N]$, multiply together and get the θ's;

(4) calculate W_{BN}, P_{BN};

(5) substitute in (9).

In general, this will not be a solution. One must then guess another ω, and try again. From the size of the remainder one can soon close in on the proper value.

(6) Do for enough values of k to get a family of $\omega(k)$ or equivalent curves.

Since all the numerical results to be presented are either group or phase velocity as a function of period, Figure 3 shows the results for an isothermal atmosphere in this new plot, as a point of reference.

In Figure 4 (from Pfeffer, 1962), results are shown for Pekeris' atmosphere, comparing his analytic solution with a numerical calculation in which the constant lapse rate has been approximated by 20 isothermal layers. The agreement can be seen to be very good, indicating we have not introduced any serious errors by our approximation method.

This was the only justification given by Pfeffer (1962). Hines (1965) expressed doubts about the validity of the isothermal layer approximation procedure, primarily because terms involving vertical derivatives of scale height (or c^2) were neglected. Recently Pierce (1966) has shown that the procedure can be rigorously justified. He remarks that the formulation by P or PH is equivalent to the expression he derives, and is accurate so long as c^2 does not change too greatly over a layer height. As he presents no criteria for accuracy, increasing the number of layers is probably still the best method of assessing accuracy.

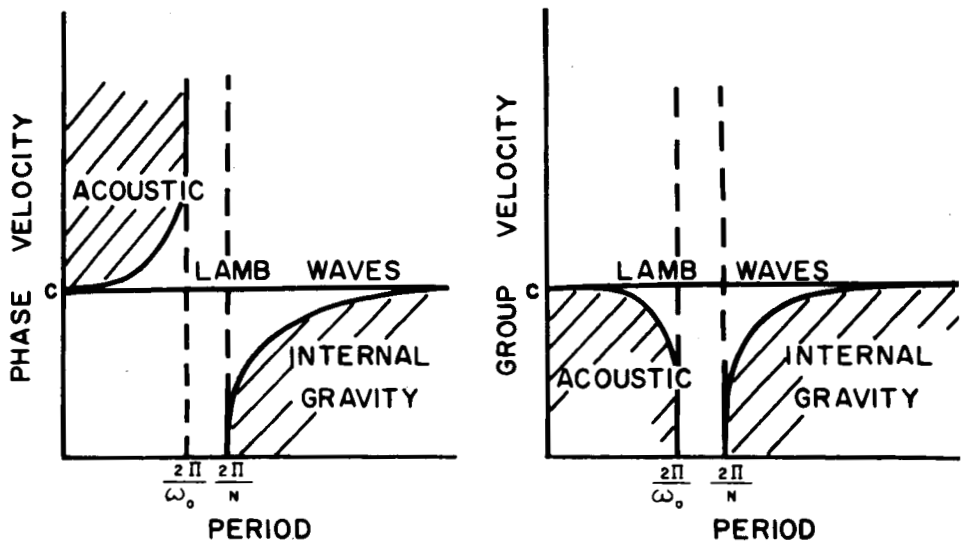

Fig. 3. Group velocity and phase velocity as a function of period for an isothermal atmosphere.

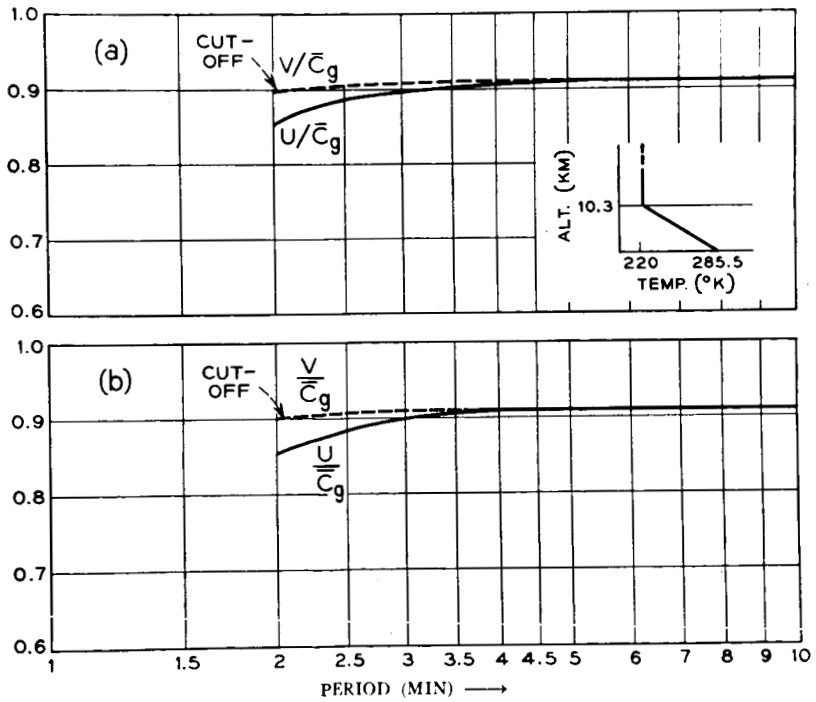

Fig. 4. (a) Variation of $U/\bar{c}_g$ and $V/\bar{c}_g$ with period for Pekeris' two-layer model atmosphere, calculated by the matrix procedure using 20 isothermal layers to represent the vertical variation of temperature in the troposphere. $\bar{c}_g$ is the sound speed at the ground. The model is shown in the insert.

(b) Variation of $U/\bar{c}_g$ and $V/\bar{c}_g$ calculated analytically by Pekeris (1948). (After Pfeffer, 1962)

3. Hueristic Results for Simple Atmospheres.

3.1 Pekeris' Model Atmosphere

Turning now to the results themselves, we see that, as implied by Fig. 2, we have a short period cut off. We also see that for long periods, the group and phase velocities approach a speed $\sim .91$ that of the sound speed at the ground - corresponding to a temperature of 235°K. These long waves "feel" both stratosphere and troposphere, and perform on averaging.

3.2 Yamamoto's Model Atmosphere

The observation of waves with period below the cut off suggested that the high temperature region of ozone absorption should be included. In Fig. 5 we see the temperature altitude curve used by Yamamoto (1957). In Fig. 6, taken from Pfeffer and Zarichny (1962) (PZI), we see the calculated U and V curves plotted against period. The short period cut off has vanished, as we expect.

Also interesting is how closely the velocity-period curve is given by the crude calculations based on the 4 thick isothermal layers. We can understand this by considering that for short period (short wavelengths) the waves are mainly confined to a single layer, while the longest ones sample large distances, and the details of the structure do not affect them. The discrepancies are largest near $\lambda \approx 20$ km which is of the order of the layer thicknesses.

The next two figures, also from PZI, illustrate the effect of a warm thermosphere. There are three interesting features:

(1) The thermosphere affects primarily the longest period waves. This is to be expected - the longest wavelengths penetrate furthest into the thermosphere.

(2) Inverse dispersion may occur - i.e. speed decreasing with increasing period.

(3) A long period cut off may occur. This is illustrated graphically in Fig. 9.

Fig. 9 shows the region of propagating ("cellular") solutions in the hot thermosphere by shading. Solution in the lower atmosphere which lie in these regions would not be trapped. The formation of modes (see next section) means only certain solutions are propagated in the lower

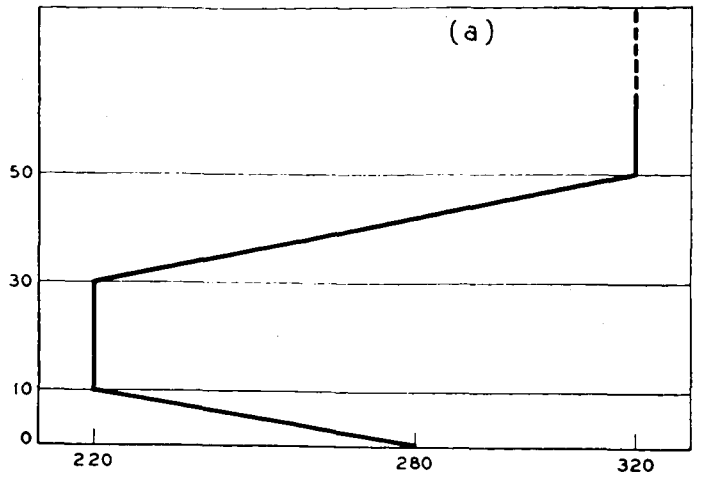

Fig. 5. Yamamoto's model atmosphere. (After Pfeffer and Zarichny, 1962)

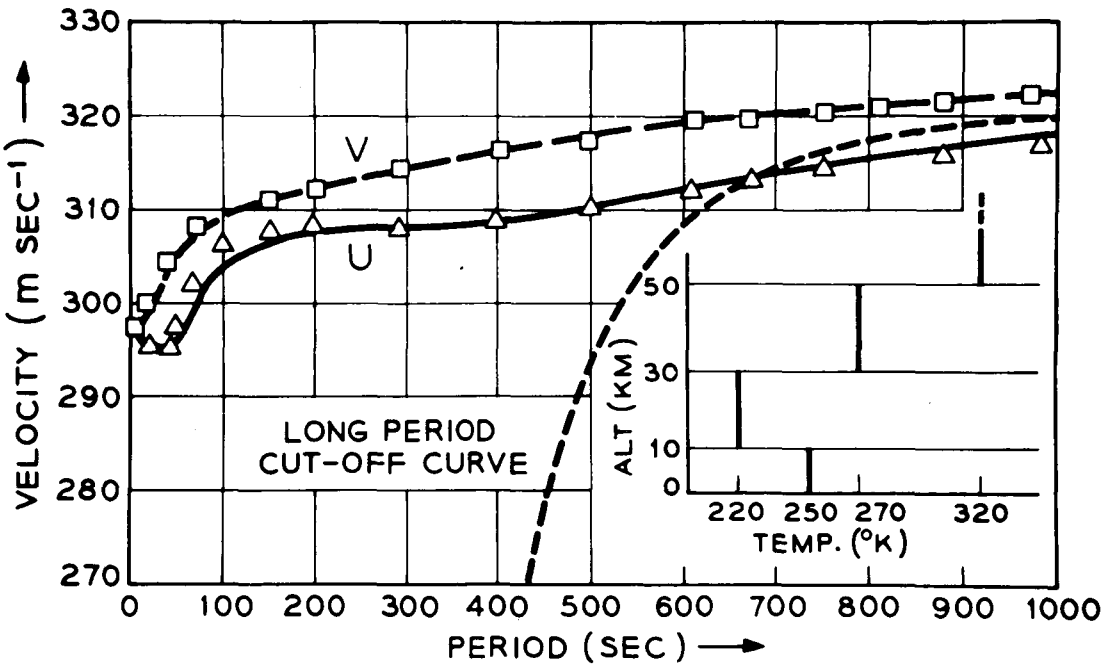

Fig. 6. Variation of group velocity (U) and phase velocity (V) with period for the fundamental mode for each of two four layer models. The curves are for the atmosphere shown in Fig. 5. Squares and triangles are for the four isothermal layers shown in the inset. The temperature of each layer is the mean of the corresponding layer in Fig. 5. The dashed cut off curve represents the boundary between cellular and non-cellular solutions in the infinite layer. (After Pfeffer and Zarichny, 1962)

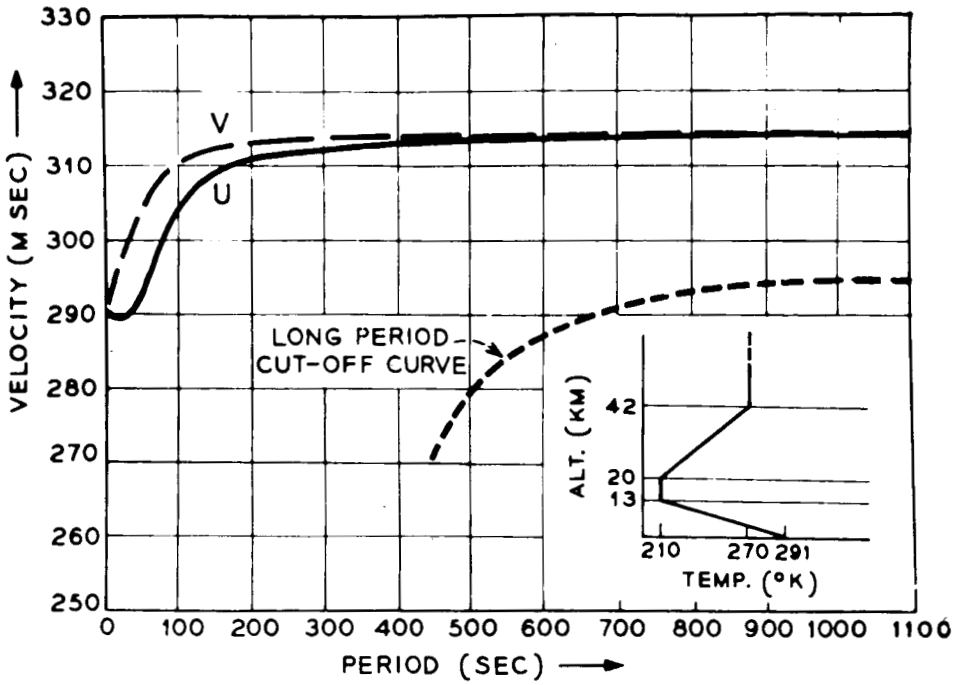

Fig. 7. Variation of group velocity (U) and phase velocity (V) with period for the fundamental mode for the "four-layer" model atmosphere shown in the inset. (After Pfeffer and Zarichny, 1962)

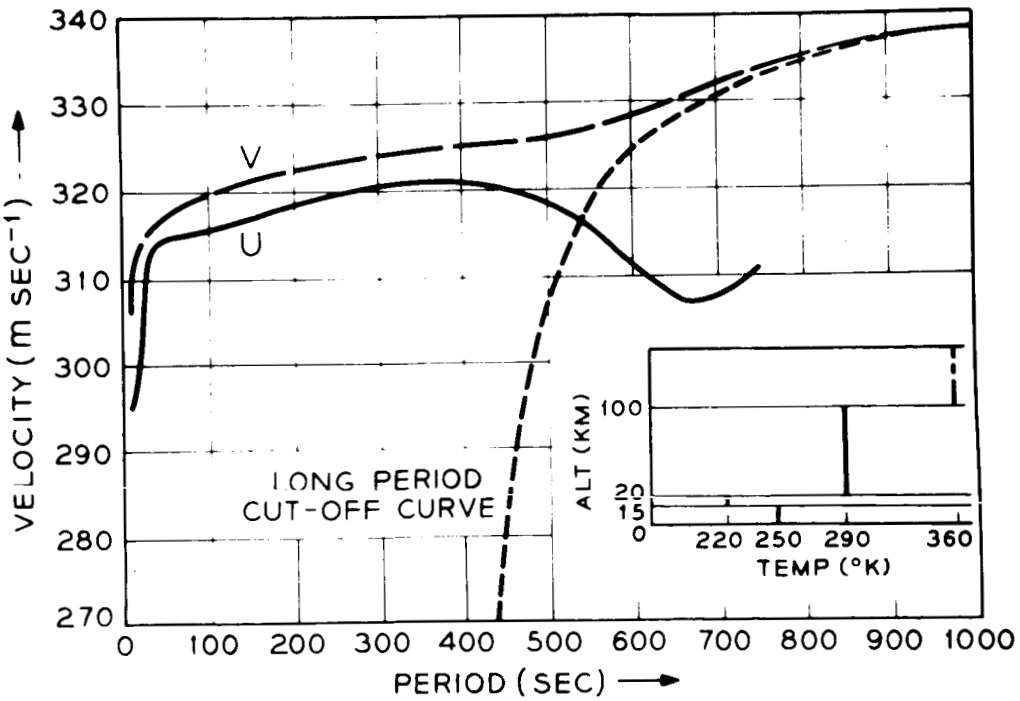

Fig. 8. Variation of group velocity (U) and phase velocity (V) with period for the fundamental mode for the four layer atmosphere shown in the inset.

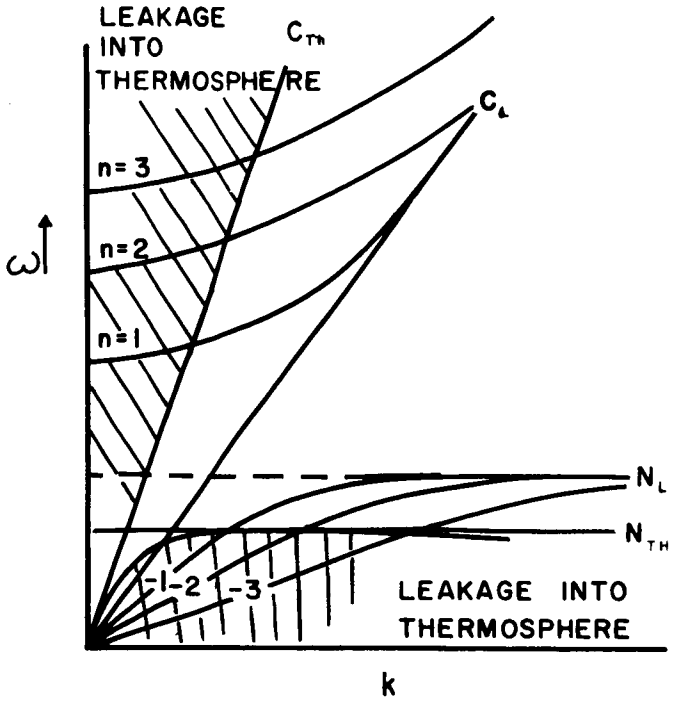

Fig. 9. Schematic illustration of long period cut off by a hot thermosphere. Shaded areas represent cellular solutions in thermosphere, and absence of trapping. Lines are mode solutions described in next section.

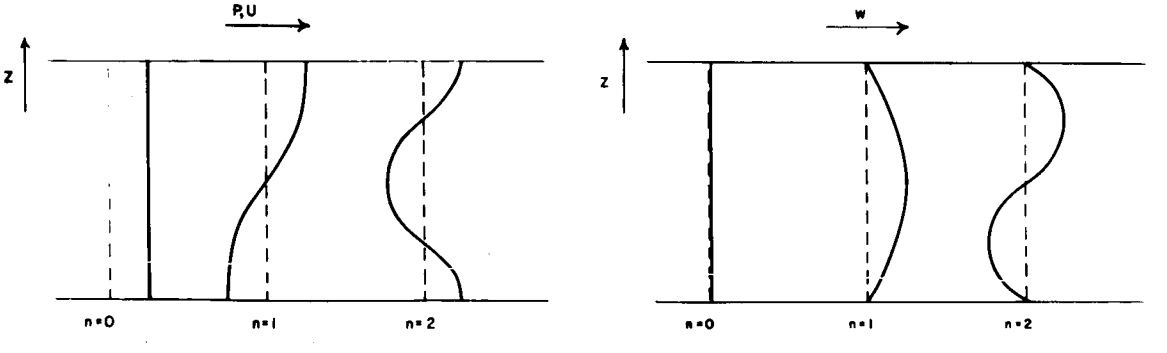

Fig. 10. The dependence of fluctuating pressure and velocities across a guide with perfectly reflecting rigid boundaries, for the first few modes. (After Budden, 1961)

atmosphere. These are illustrated by the lines labeled n = 1, 2, 3, etc. Each of these and the fundamental has a long period cut off.

4. A Brief Digression on Wave Guide Theory.

The rigid lower boundary will act to reflect a wave front incident obliquely upon it, and we have seen that an upper structure that reflects or refracts waves incident obliquely on it back to the surface also exists. The possibility of forming a wave guide mode of crossing wave fronts exists. In addition, we can have waves for which both reflections take place above the surface. A very lucid treatment of this subject, developing electromagnetic and acoustic theory together, is given by Budden (1961). We will follow his treatment in the first part of this section.

Consider a wave guide whose boundaries are the planes z = 0 and z = h, with reflection coefficients

$$\begin{aligned} R_g(\theta) &= e^{-2ik\chi t} && z = 0 \\ R(\theta) &= e^{-2ik\chi t} && z = h \end{aligned} \qquad (1)$$

for a plane wave whose normal makes an angle θ with either boundary.

If some quantity obeying the wave equation is given by

$$F_1 = F_0 e^{-i(kx+nz)}$$

After reflection at z = h, and return to the lower boundary

$$F_2 = R(\theta) F_0 e^{-i(kx-nz)} e^{-2inh}$$

(the last factor takes account of phase change of the wave in traveling up to and back from the upper boundary). After F_2 is reflected from the bottom,

$$F_3 = R_g(\theta) R(\theta) e^{-2inh} F_1.$$

The condition that a wave guide exists is that F_1 and F_3 must be identical. This requires

$$R(\theta) R_g(\theta) e^{-2inh} = 1. \qquad (2)$$

For a plane of perfect reflection, R = 1. Thus, if upper and lower surfaces are rigid boundaries,

$$e^{-2inh} = 1$$

or

$$nh = m\pi \tag{3}$$

where m is an integer, the mode number.

Those modes are similar to TM electromagnetic modes, and are shown in Fig. 10 (after Budden, 1961). Note that an m = 0 mode is possible here.

A free surface is one which cannot sustain any change of pressure. For displacements, R = -1. Again we find nh = mπ, but a detailed study of the equations indicate that they are like TE electromagnetic modes. Their properties are shown in Fig 11 (after Budden, 1961). Here no m = 0 mode is possible,

The more usual geophysical case is given by one rigid and one free boundary. Here we find

$$nh = (m - 1/2)\,\pi \tag{4}$$

and again no m = 0 mode is possible. Here u and w are shown in Fig. 12 (from Budden, 1961). The particle motions are shown in Fig. 13.

We can write

$$K \sin\theta = n \tag{5}$$

where K is the wave number along the direction of a wave normal. Then

$$Kh \sin\theta = (m - 1/2)\pi \tag{6}$$

has a minimum frequency of propagation, corresponding to sin θ = 1, and, with $K_c = \omega_c/c$

$$\omega_c(m) = \frac{(m - 1/2)\,\pi c}{h} \tag{7}$$

$$\text{In general } \frac{\omega_c}{\omega} = \sin\theta, \tag{8}$$

and noting that the wave fronts move in the x direction so that kx - ωt = K cos θx - ωt = const., the phase velocity is given by

$$V = \frac{\omega}{k} = \frac{\omega}{K\cos\theta} = \frac{c}{\cos\theta} = c(1 - \omega_c^2/\omega^2)^{-1/2} \tag{9}$$

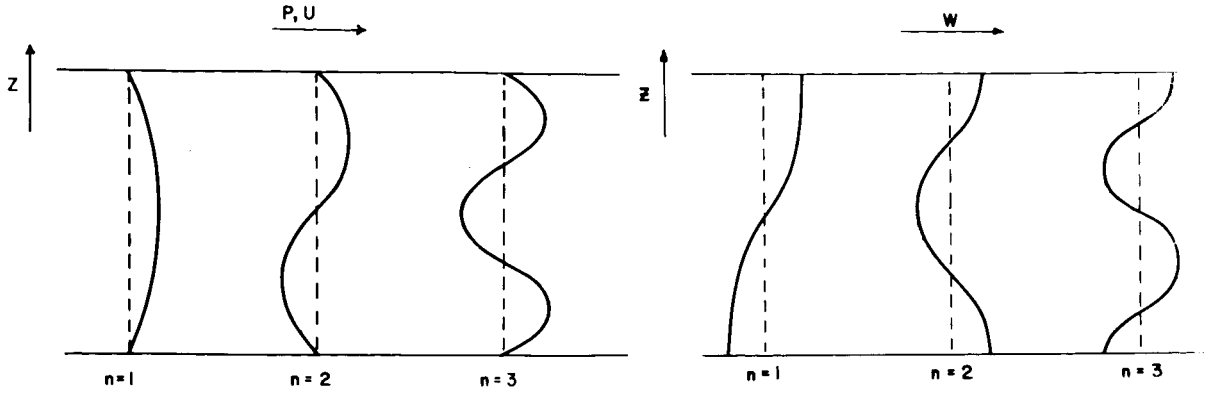

Fig. 11. The dependence of perturbation pressure and velocities across a guide with perfectly reflecting free boundaries, for the first few modes. (After Budden, 1961)

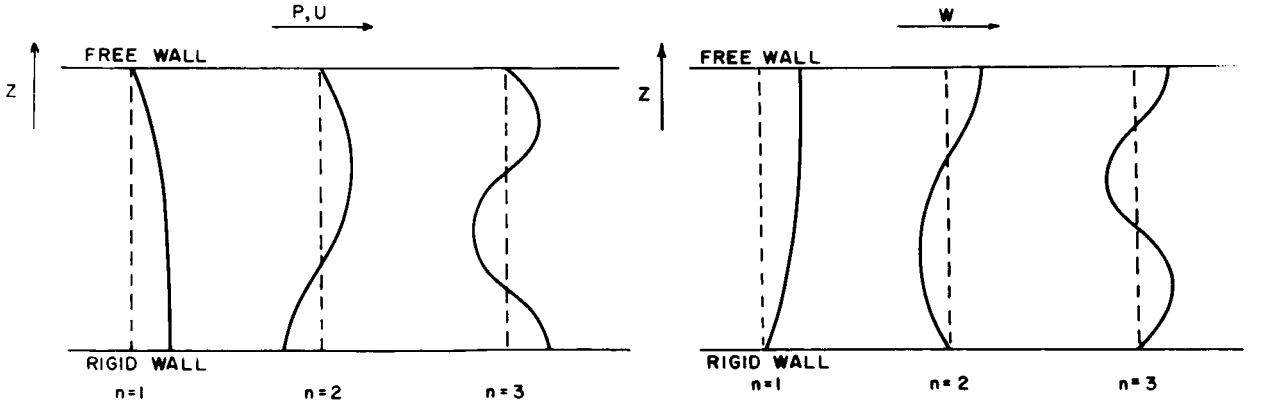

Fig. 12. The dependence of perturbation pressure and velocities across a guide with one rigid, one free boundary, for the first few modes. (After Budden, 1961)

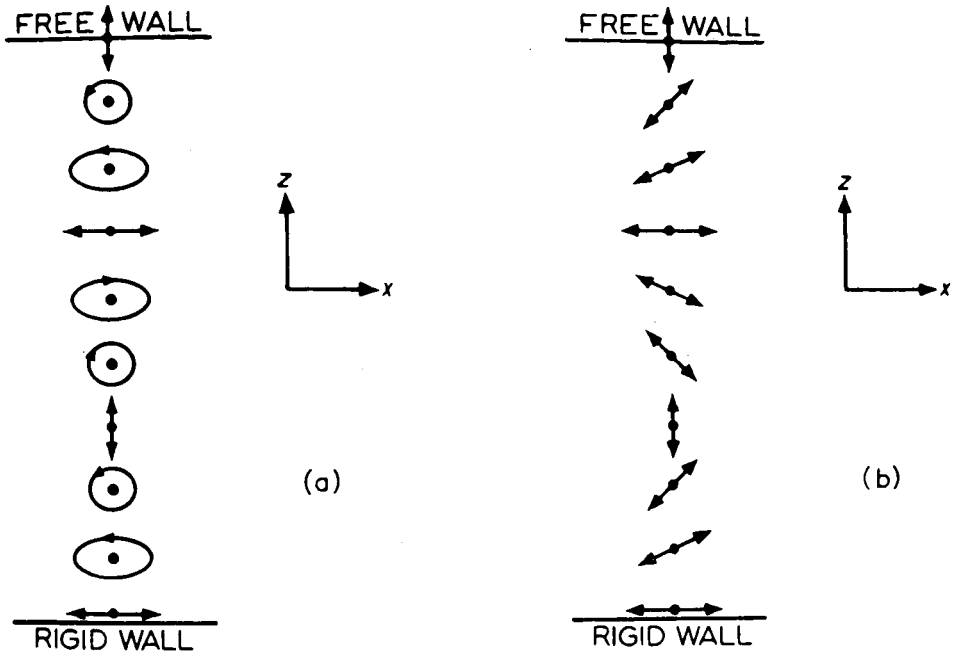

Fig. 13. Particle orbits for a sound wave of mode 2 in a guide with one rigid, one free boundary. Figure (a) is for mode with frequency greater than cut off (propagation) figure (b) for frequency below cut off (evanescent).

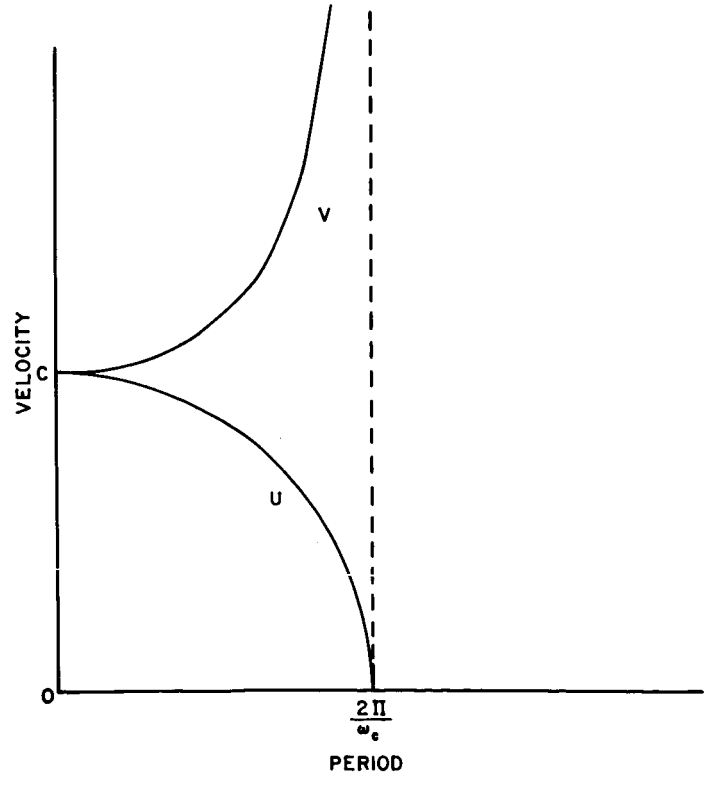

Fig. 14. Phase velocity and group velocity as a function of period for any mode in a wave guide with perfectly reflecting walls. Here ω_n is the cut off frequency.

The group velocity is $U = c\left(1 - \frac{\omega_c^2}{\omega^2}\right)^{1/2}$ (10)

This behavior is shown in Fig. 14.

In the general case, from (1) and (2)

$$nh = \chi(\theta)\uparrow + \chi(\theta)\downarrow + m\pi \tag{11}$$

For stratified media, Tolstoy (1954) shows how reflection coefficients may be calculated for a layered medium, and how this formulation may be generalized to a medium with continuously varying parameters. In general, χ depends on ω and k. For thick layers (approximating half spaces) the method of calculating reflection coefficients has been discussed in the first lecture.

Equation (11) makes very clear that there are two sources of dispersion:

(1) Dispersion appearing in the equations for n. This depends on internal fluid resonances, and appears in unbounded fluids. Tolstoy (1963) has termed this structural dispersion.

(2) The interference between upward and downward traveling waves leads to dispersion. This has been termed geometric dispersion by Tolstoy (1963).

Tolstoy also shows that for exponential modes ($n^2 < 0$), m = 0. There is then no vertical phase variation, the wave fronts are normal to the planes of stratification. These are the Lanb type waves, which thus play the role of the zeroth acoustical mode. This is the wave which has been discussed until this point. Following PZI, we shall refer to this as the fundamental.

The effect of the boundaries is to "quantize" the vertical wave number n, forcing it to assume (non-zero) integer values. This is shown for the case of the ocean in Fig. 15 (from Eckart, 1960). Although this is simpler than the atmosphere, it illustrates the general behavior

5. Higher Modes in Simple Atmospheres.

We see in Fig. 15 that there are several discrete ω's corresponding to a single k, which are all solutions. These have been calculated by PZI, for Yamamoto's atmosphere. Since the warmest layer is the upper half-space, there are long period cut-offs for these modes.

It is more instructive however to consider in greater detail the series of calculations by Pfeffer and Zarichny (1963) and Pfeffer (1964)

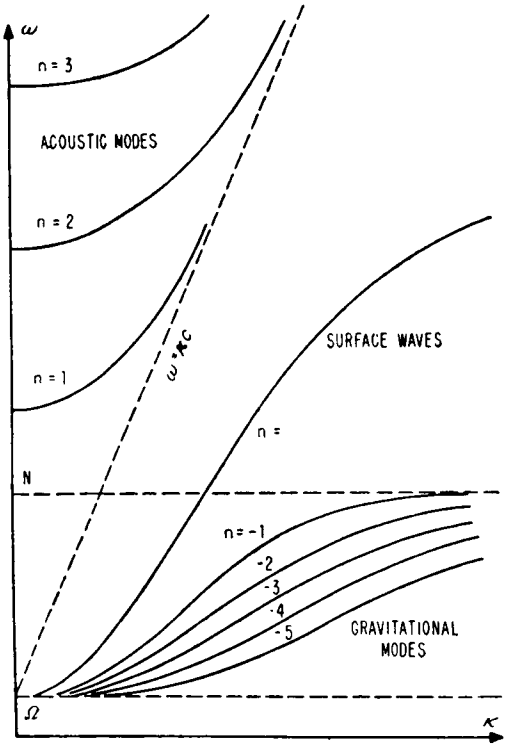

Fig. 15. ω vs k diagram for the general case of an ocean of constant depth and constant N, ω_0, and c. Low frequency region near the earth's rotation frequency Ω is not considered here. (After Eckart, 1960)

on the COSPAR atmosphere, which is shown in Figure 16. In this section we shall consider the higher modes for the COSPAR atmosphere terminated at 52 km by an isothermal half space. Later we will consider the effects of termination at 110, 300, and 700 km.

In the case of 52 km termination there is just one temperature minimum, or conventional sound channel. The fundamental and higher modes are presented by Pfeffer (1964) and shown in Fig. 17. Note that we again have long period cut-offs in both acoustic and gravity modes. This is due to longer wavelengths in the duct becoming incident at higher angles on the half space, until they are no longer returned. The fundamental is not cut off because the upper half space is slightly cooler than the surface. The longer periods for the fundamental have higher velocities than the shorter periods.

Figure 18, also from Pfeffer (1964) shows the location of the kinetic energy for the various modes at various periods. (The temperature profile is to the left.)

Taking the fourth acoustic (4A) mode as an example, we note the four nodal planes at 16 and 21 sec periods, and the limited energy along the temperature incline. At 25 seconds, the energy curve is not coming back to zero at the top. Energy is penetrating on into the half space, and not being returned. This is the cut-off period for this mode. Here the ducting seems to be between the two regions of high temperature.

On the other hand, the fourth gravity mode has only 3 nodes. Again mode cut off is signalled by the sudden increase in half space energy - here at 340 sec period.

The behavior of the gravity modes is less easily understood than the acoustic modes. However, we note the tendency to concentrate in the region of large N (along the temperature incline). This region appears to be the duct for the first gravity mode at 288 seconds.

At 303 seconds, where the wavelength is greater, the lower reflecting region seems at the top of the region of negative temperature gradient, and eventually at the ground.

The fundamental energy, at short periods, is concentrated in the low speed channel - where we saw the acoustic energy was. Note the similarity between the 85 sec, Fundamental and 1A at 80 seconds, and the difference at

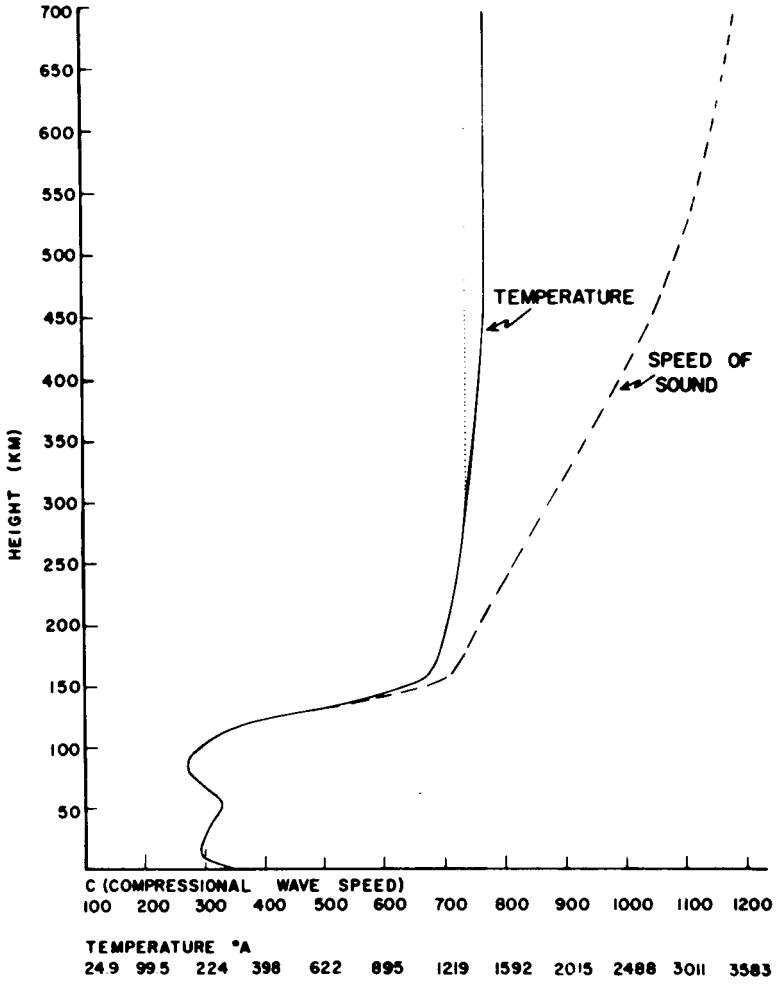

Fig. 16. Average vertical variation of absolute temperature in the atmosphere estimated by the Committee on Space Research (solid curve) and related compressional wave speed (solid curve up to 74 km and broken curve above this level) in m sec^{-1}. (After Pfeffer and Zarichny, 1963)

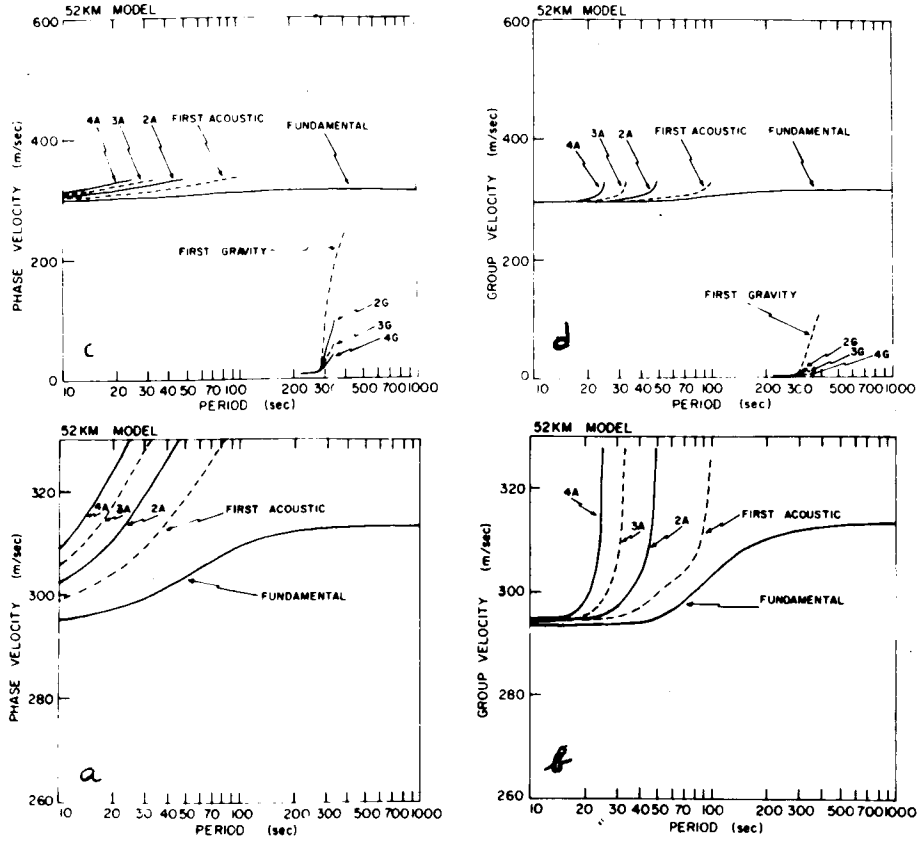

Fig. 17. Phase velocity and group velocity for the 52 km COSPAR atmosphere. (After Pfeffer, 1964)

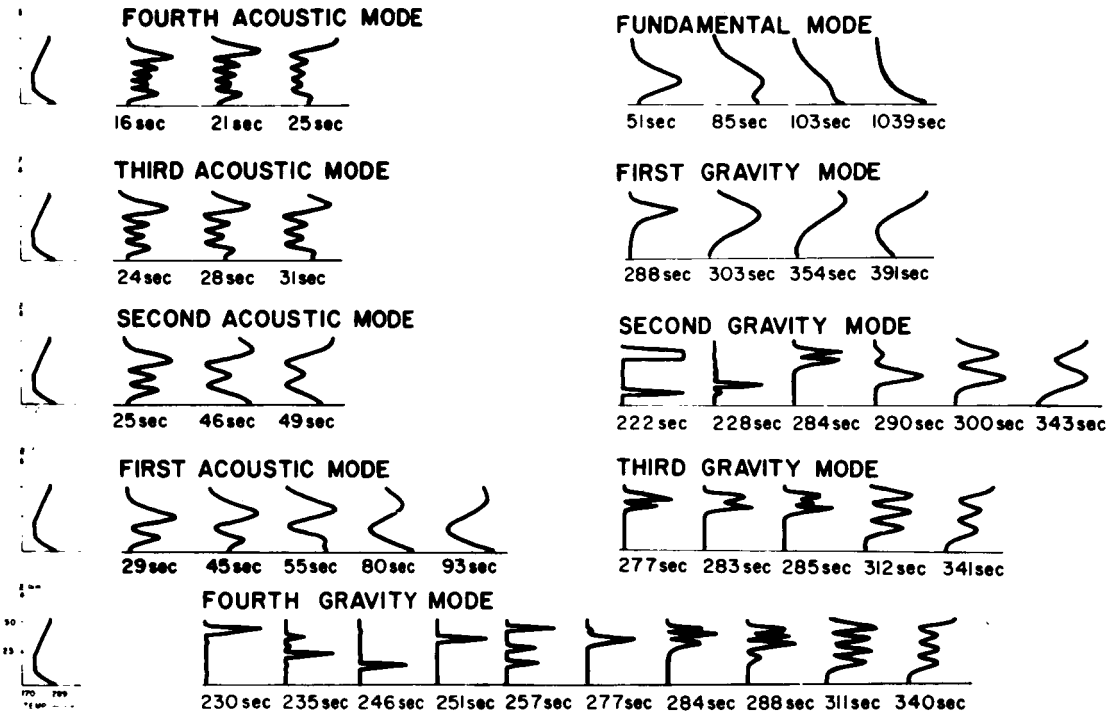

Fig. 18. Kinetic energy density as a function of height for the 52 km COSPAR atmosphere. (After Pfeffer, 1964)

103 and 93, respectively. At long periods its exponential character becomes very clear with energy concentrated at the surface. It is the higher speed at the warm surface than in the cold channel which increases the fundamental velocity with increasing period.

The real atmosphere possesses two temperature minima, of course, but the modes of the lower channel are very helpful in understanding the modes of the whole atmosphere.

6. Ducting in an Atmosphere with Two Sound Channels.

PZI noted that important characteristics of waves recorded at the earth's surface due to explosions in the lower atmosphere might be strongly influenced by the mesospheric temperature minimum, and that firm conclusions about wave propagation in the atmosphere required theoretical calculations based on models with two sound channels. Velocity-period relationships for atmospheres with two minima have been obtained by Gazaryan (1961), Weston (1962), Press and Harkrider (1962) and Pfeffer and Zarichny (1963) (hereafter denoted as PZ II).

6.1 Effect of termination height on the Fundamental mode.

PZ II calculated the properties of the fundamental and compared the results when the atmosphere was terminated by an isothermal half space at 52, 110, and 130 km. The results are shown in the next figure (19). An immediately comprehensible effect is the lower short period velocity for the 110 and 130 km atmospheres, due to the concentration of short period acoustic-like waves in the upper (slow) sound channel. We also note the high velocity of long-period waves, due to the influence of the high temperature, high speed region, between 110 and 130 km.

In the upper portion of figure 20 is a plot of kinetic energy density against altitude. It shows that, for short periods, the kinetic energy density of the waves is concentrated in the stratospheric sound channel for the 52 km model, and in the mesopause channel for the 110 and 130 km models.

The intermediate period waves (150-290 sec), which have horizontal wavelengths from 46-94 km, will not fit in either channel. These are bound to the rigid surface of the earth, with kinetic energy decreasing exponentially with height. These wave speeds are not influenced significantly by temperature distribution above the stratopause. The previous figure showed

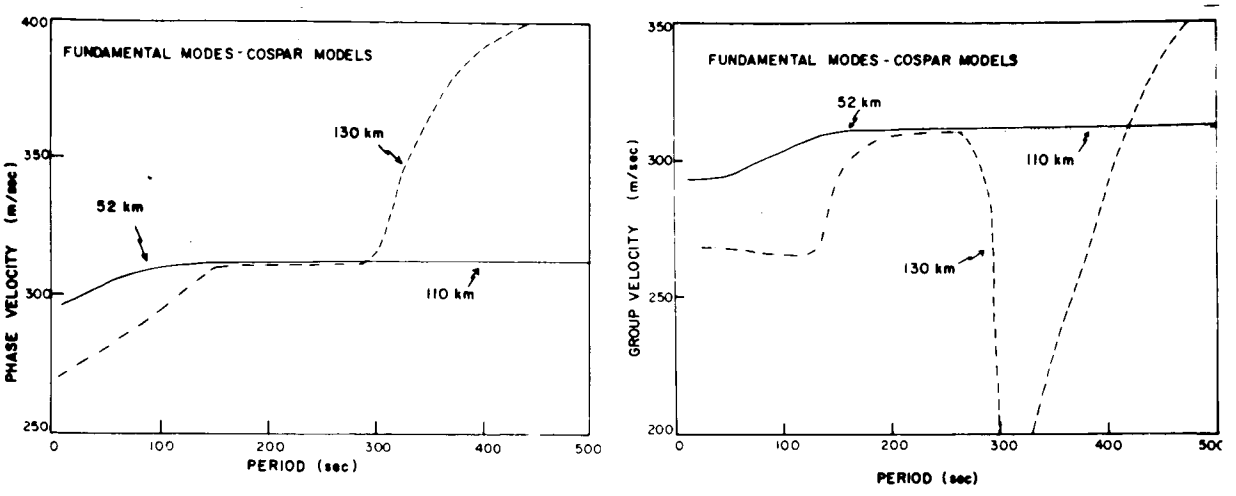

Fig. 19. Theoretical velocity-period curves for the fundamental mode of the COSPAR atmosphere for three termination heights. (After Pfeffer and Zarichny, 1963)

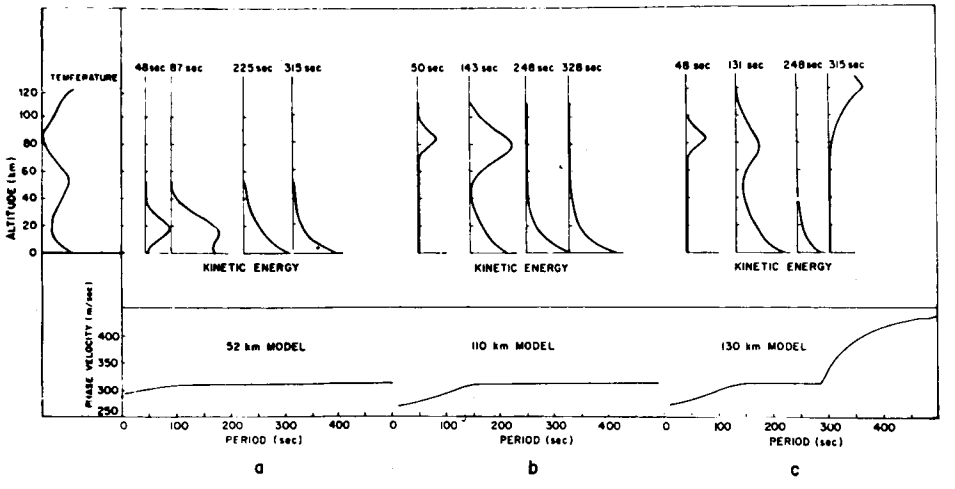

Fig. 20. Vertical profiles of the kinetic energy of the waves per unit volume at selected periods. The vertical scale and the temperature profile are shown on the left hand side of the figure. The phase velocity curves are shown at the bottom for the three models. (After Pfeffer and Zarichny, 1963)

that the group and phase velocities nearly coincide over this range of periods.

For periods > 290 sec, the waves are sensitive only to major differences between the lower and upper atmospheres. The kinetic energy per unit volume decreases exponentially with altitude in the 52 and 110 km models, but is confined to the upper atmosphere in the 130 km model. The exponential decrease with height in the first two cases is characteristic of all models in which the temperature maximum is at the surface.

6.2 Modes in the 300 km COSPAR Atmosphere.

Proceeding as before to find all ω's associated with a particular k, PZ II shows, for the 300 km COSPAR atmosphere, the velocity-period curves shown in Fig. 21.

Here we see the great complexity of 5 acoustic and 5 gravity modes, with greater detail on the inset. Not shown,the fundamental has a cut-off for period > 1000 sec, due to the warm thermosphere and all other modes cut off before this. This, of course, refers to the surface, and only means that energy is leaking up from the lowest layers. The cut-offs are shown more clearly in Fig. 22 for a similar atmosphere, calculated by PH, although their fundamental does not cut off. Note that S_0 is what we have called the fundamental, S_1 is the first acoustic, etc., while GR_0 is what we have called the first gravity mode.

In Figure 23 we see the same calculation on an expanded velocity scale, and compared to the 52 km "fundamental" and first acoustic mode.

Note that the phase velocity curves for the fundamental mode, first gravity mode and the first three acoustic modes are step-like functions, with rather steep short and long period branches, separated from one another by nearly horizontal intermediate period branches.

The group velocity curves have broad maxima, separated from one another by small but distinct intervals of period. The most surprising point is that selected horizontal portions of the phase velocity cuves coincide with the phase velocity curve of the 52 km model atmosphere, while other horizontal portions coincide with the first acoustic. The plateaus of the group velocity curves coincide with the 52 km group velocity curves. Not only do the horizontal portions lie along common lines, but the vertical portions of the curves for different mode numbers are seen to be very closely aligned.

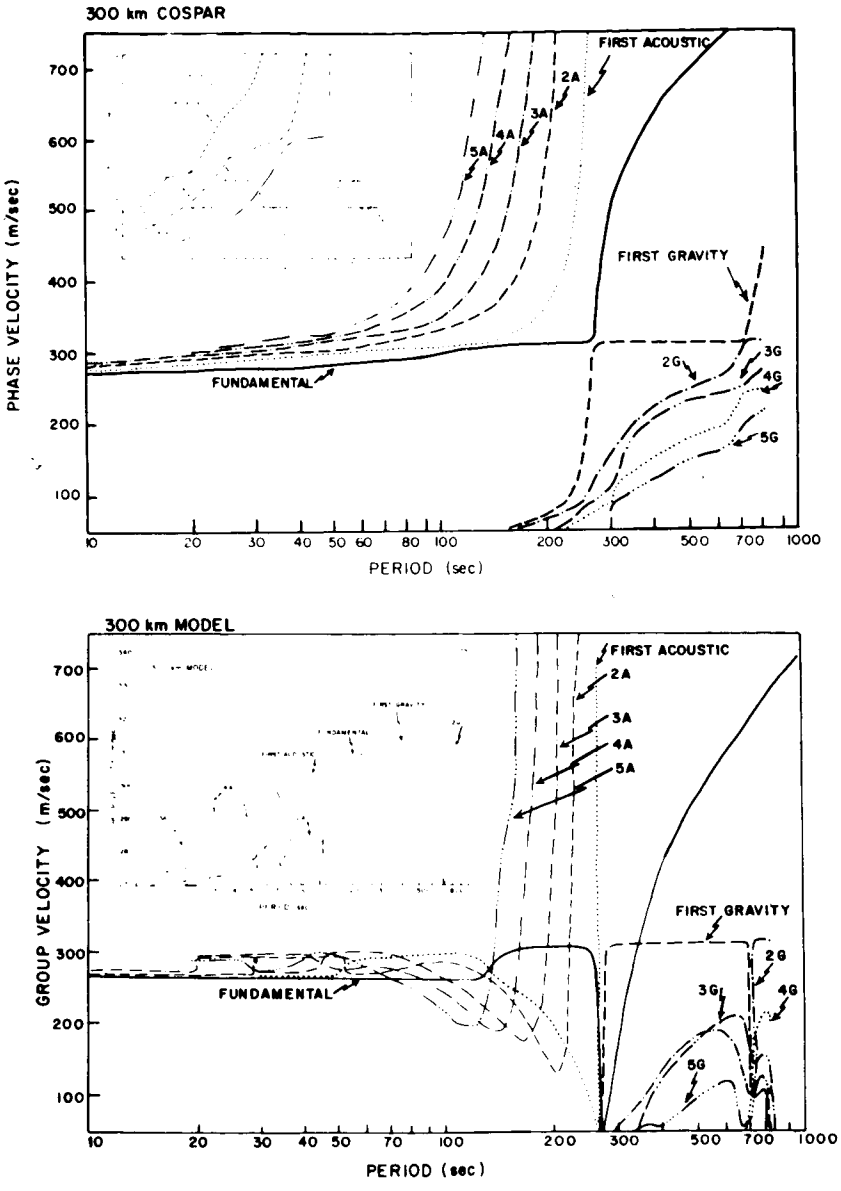

Fig. 21. Dispersion curves for the fundamental mode, the first five acoustic modes, and the first five gravity modes. (a) Phase velocity vs. period; (b) group velocity vs. period. The details of the velocity-period relationships between 270 and 340 m sec-1 are given in the insets. (After Pfeffer and Zarichny, 1963)

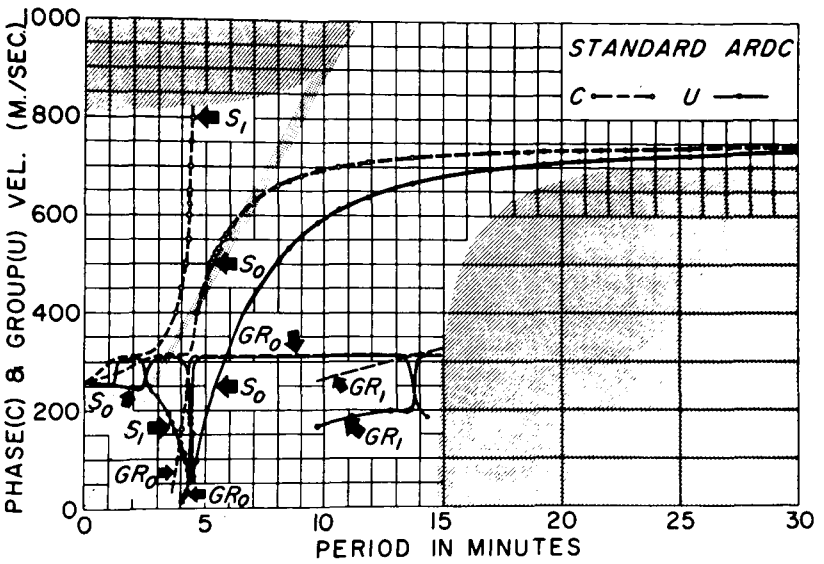

Fig. 22. Phase and group velocity for the ARDC standard atmosphere. Shaded regions correspond to cellular solution in the thermosphere. (After Press and Harkrider, 1962)

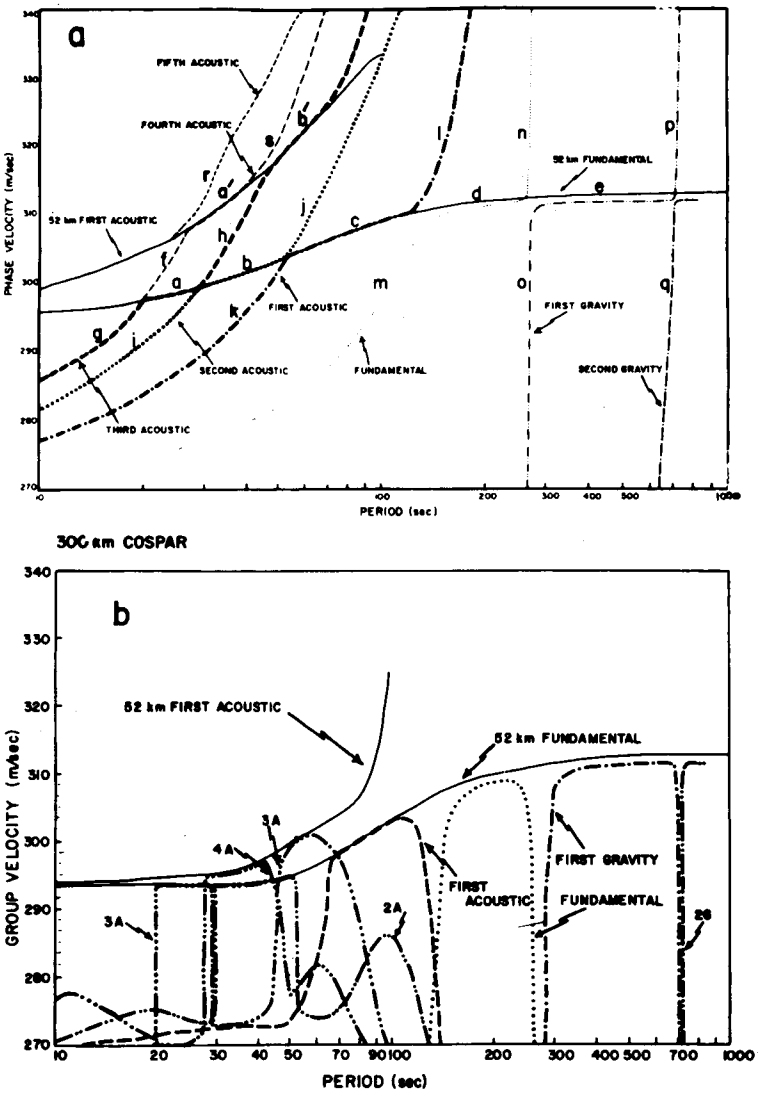

Fig. 23. Comparison between dispersion curves for the 52 km and 300 km models, showing the quasi-horizontal portions of the phase and group velocity curves for the 300 km model coincide with the solutions for the 52 km model. (a) phase velocity vs. period; (b) group velocity vs. period. The small letters in the upper figure refer to points at which vertical profiles of kinetic energy were calculated and are shown in Fig. 26. (After Pfeffer and Zarichny, 1963)

PZ II agrees with the conclusion of PH that "the character of the propagating disturbance at any time is perhaps better represented by pseudo-dispersion curves formed by segments of several modes". These horizontal portions are clearly strongly dependent on the lower sound channel and the warmer regions around it. PH present all the properties of their dispersion curves which are unaffected by what happens above 100 km, and these are, in agreement with PZ II, the horizontal portions. The vertically rising portions of the curves depend on the atmosphere above 110 km, and therefore we would not expect them to be strongly excited by near surface disturbances, whether of the lee-wave or point impulse type. In addition, amplitudes are proportional to $(dU/dP)^{-1/2}$ (where P is the period); again, we expect little surface amplitude at these periods.

This suggests that one might look for these holes in the spectrum on observed barograms. PZ II does this in a very ingenious manner, and presents evidence from recorded barograms that narrow intervals of period are missing for periods where these vertical curve segments are.

The effect of latitudinal and seasonal variations have been calculated by PZ II and PH. However, these affect mainly the lower atmosphere, and thus say little about the wave spectrum above the second sound channel. Variations in this region have been incorporated by PZ II, whose results are shown in Figure 24. Note that the COSPAR atmosphere appears to allow higher frequency (shorter period) waves to leak upward in both the fundamental and first gravity modes. It would be interesting to look for a variation in wave spectra at ionospheric heights with sunspot cycle, to see if there is this tendency for high solar index to go with longer period waves.

6.3 Mode interaction.

Let us take a moment to try to understand this phenomenon of mode segments corresponding to portions of larger curves. Tolstoy (1956) has discussed the technique of separating a complex layered waveguide into two partial waveguides along a nodal surface. Then free boundary conditions are applied along this surface, the two guides are solved separately, and then overlaid. For those values of ω having the same k's as solutions, this ω, k is applicable to the complete wave guide. If the mode number of the lower guide is ℓ, the upper u, and of the complete guide m, then

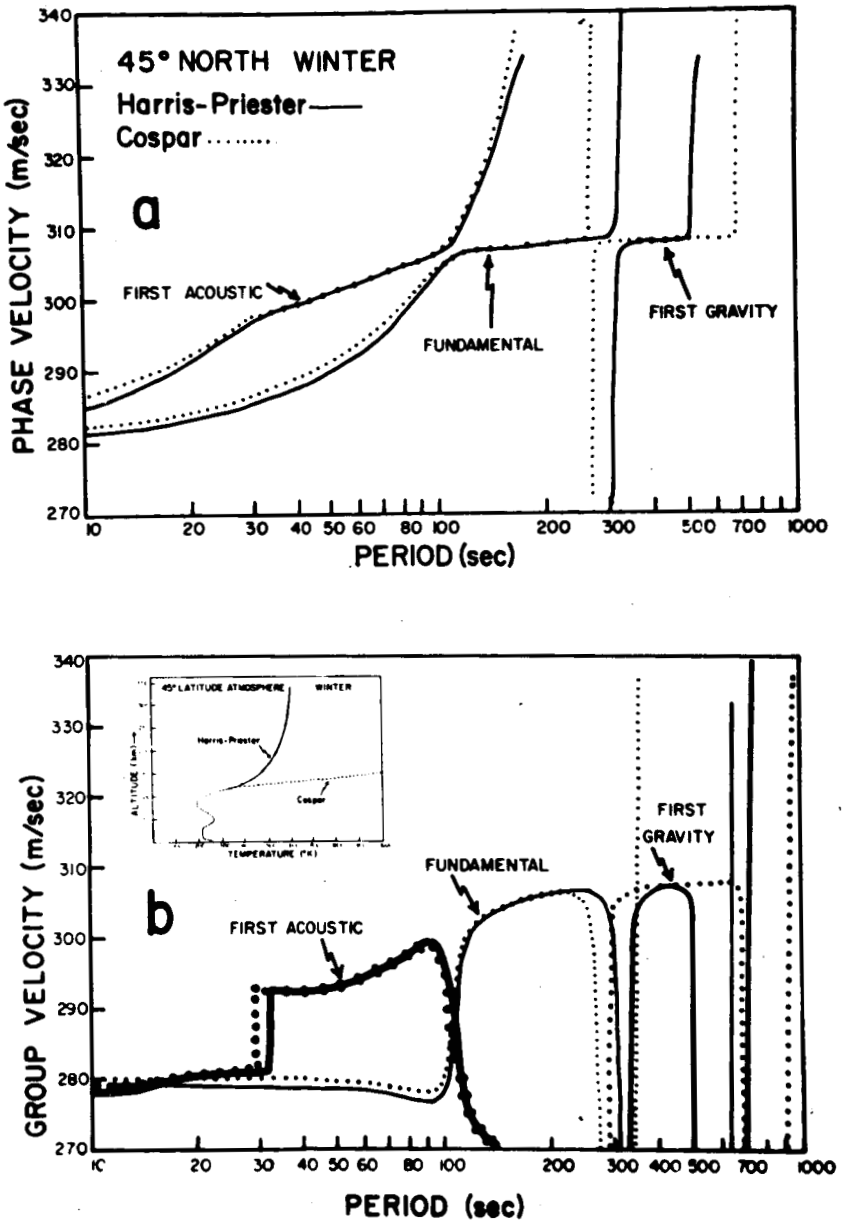

Fig. 24. Dispersion curves for model atmospheres consisting of the temperature structure at 45°N in winter up to 90 km merged with a nighttime atmosphere for a period of minimum solar activity due to Harris and Priester (solid curves) and with the mean COSPAR atmosphere (dotted curves).
(a) phase velocity vs. period, (b) group velocity vs. period. The atmospheres are shown in the inset. (After Pfeffer and Zarichny, 1963)

$$\ell + u = m \qquad (1)$$

Considering a temperature structure like that in Fig. 16, let us imagine a boundary surface through the stratopause region at 52 km. Now considering separately the ω, k solutions of the upper and lower guides, we find that the vertical curves correspond to sections of acoustic modes of the upper channel, while as noted, the horizontal portions are similar to the fundamental and first acoustic of the lower channel. We can transform the PZ results into the ω-k plane as indicated in Fig. 25.

Letters have been put in, corresponding to the appropriate portion of the PZ II curves. The curves have also been labeled with mode numbers u and ℓ for the two half-wave guides. Where intersections occur, solutions for the whole wave guide are possible, with m given by (1).

In common with Tolstoy's (1955, 1956) findings about elastic wave propagation, the modes of the complete wave guide follow a path made up approximately of segments of upper modes alternating with segments of lower guide modes. Consider, for example, the path beginning on u = 2. This is a solution to the whole wave guide, with m = 2, with both nodes (and we expect, the energy) in the upper channel. At the intersection (2,0) with the lower fundamental, the complete mode switches to follow the lower mode line. We anticipate energy in the lower channel now, in common with an atmosphere with no upper channel. The upper guide, with little energy concentration, is altering its solution. At the next intersection, (1,0), the complete mode again switches to the upper mode - energy is in the upper channel, and the lower channel solution is in transition to one with one mode - the lower first acoustic.

As implied above, when the complete guide mode is following an upper mode line, its characteristics are those of the upper guide, and it is strongly coupled to the upper modes; similarly, on the lower mode segments it looks like a lower mode.

This is completely corroborated by the energy density curve of PZ II (Fig. 26). Looking first at the horizontal portions of the velocity-period curves, we note the close correspondence between the energy density of the modes (written in the form m (u,ℓ)), 3(3,0), 2(2,0), 1(1,0) -1(-1,0) and the ℓ = 0 mode of the lower channel alone. Also 4(3,1) and 3(2,1) follow the ℓ = 1 line. Similarly, looking at the vertical portions, we see g, f

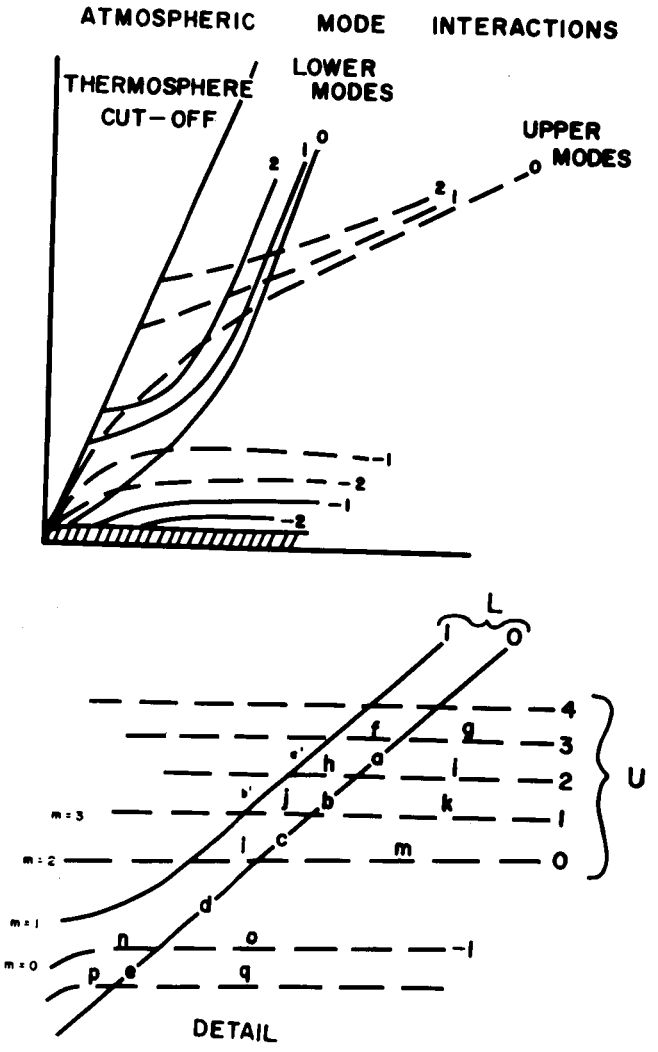

Fig. 25. Schematic diagram of mode interaction in an atmosphere with two sound channels. Lower and upper modes are for the portion of a COSPAR amosphere below and above a fictitious free surface at about 52 km.

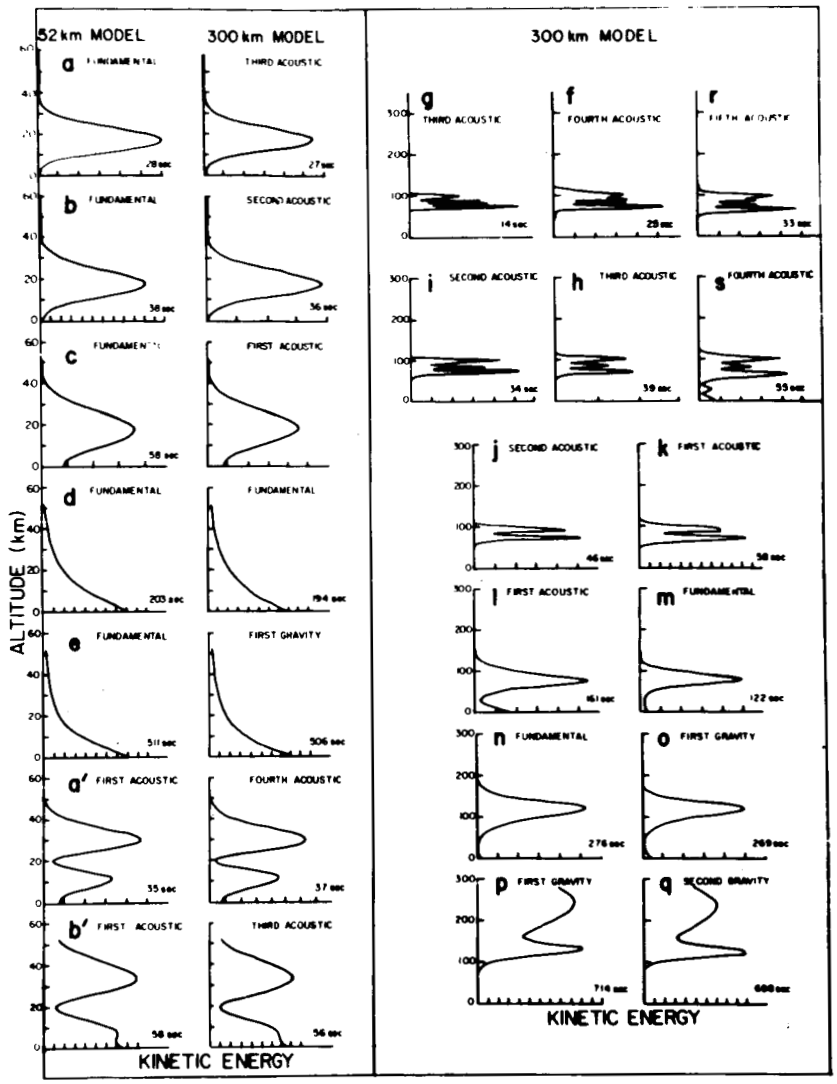

Fig. 26. Vertical profiles of the kinetic energy of the waves per unit volume. (a) comparison between profiles for the 52 km and 300 km models at the points a, b, c, d, e, a', and b' of Fig. 23; (b) comparisons among the profiles at points g, f, and r; i, h and s; j and k; l and m; n and o; and p and q of Fig. 23. Curves are normalized to have same maximum amplitude. (After Pfeffer and Zarichny, 1963)

and r are 3(3,0), 4(3,1) 5(3,2) all have u = 3, and i, h, s are 2(2,0), 3(2,1), 4(2,2) have u = 2. Note also that ℓ = 1 corresponds to one energy minimum in the lower channel, and u = 2 or 3 correspond to 2 or 3 energy minima in the upper channel. In the vertical branches, there is so little energy in the lower channel that the number of nodes cannot be seen on this scale.

Another interesting sequence is to follow the course of m = 3 and m = 2.

m = 3				m = 2			
Curve section	u	ℓ	P	Curve section	u	ℓ	P
g	3		14 sec	i	2		34 sec
a		0	27 sec	b		0	36 sec
h	2		39 sec	j	1		46 sec
b'		1	56 sec				

A further corroboration of the nature of the vertical portions of the curves is seen in Fig. 27, which is for an atmosphere with a rigid top and isothermal half-space at the surface. Since the fundamental depends upon the lower boundary for its existence, it should disappear. On the other hand, since all but the longest period waves are located below 300 km, the presence of the lid should have little effect. This is seen to be the case. The gravity modes are identified by their approach to a long period high velocity asymptote, while the acoustic modes approach infinite velocities or cut off at long periods.

One can ask for further physical insight into these points of sudden change. It appears from the formulation of Eckart (1960) that they are related to the relative positions of the points where $\omega = N(z)$ and $\omega/k = C(z)$. In his formulation of the problem, the relative positions of these points on a phase diagram determine the character of the solution. After a qualitative examination of the solutions for an atmosphere with one temperature minimum, and constant lapse rate thermosphere he remarks that when the vertical description of the solution "...contains two oscillatory segments separated by a non-oscillatory one, small changes in k and ω may produce large quantitative changes in the phase path." These changes include switching the maximum amplitude between upper and lower channels.

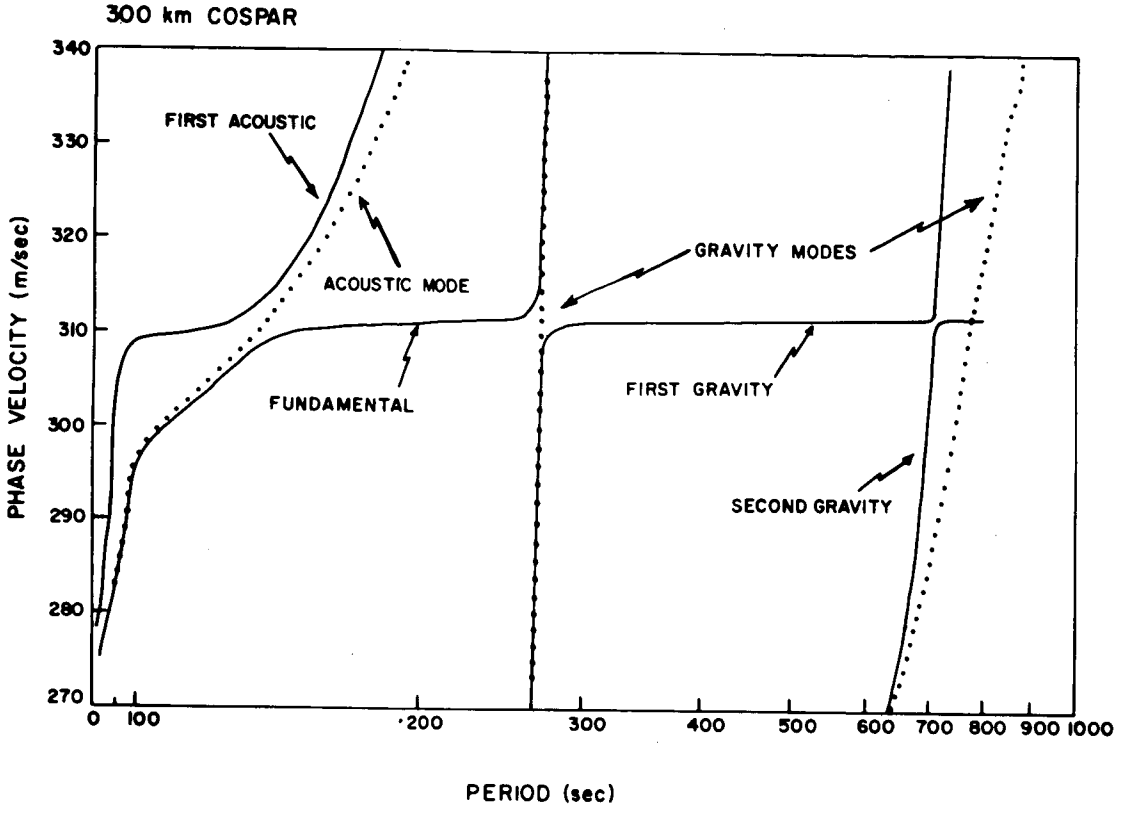

Fig. 27. Phase velocity vs. period for the COSPAR atmosphere bounded by a rigid surface at the ground and a half space above 300 km (solid curves) and for the same atmosphere with the boundary conditions reversed (dotted curves). (After Pfeffer and Zarichny, 1963)

The phase diagrams also explain the appearance of extra nodes in the numerical calculations of a given mode, since it is possible to add any number of pairs of cancelling nodes without affecting the net mode number. The application of an Eckart-type analysis of the modes of an atmosphere with two temperature minima should provide further understanding of the relevant mode interactions taking place.

6.4 Energy density.

Energy density diagrams (Figs. 26 and 28) provide quite useful information, since neither pressure oscillations nor wave motions can be observed where there is no energy.

The interesting case of pressure oscillations and simultaneous ionospheric disturbances is seen to be rare, but we quickly note possibilities at about 270 sec (F,1G), 707 sec (1G,2G) 400 to 497 sec (3G). These are also the periods we would expect to see excited by broad band sources in the lower atmosphere, like volcanic activity, earthquakes and atmospheric motions.

Similarly, the periods for which large amounts of energy are leaked into the ionosphere can be picked out - 1077 sec (F) and 720 to 800 sec (1G). These might be observable at great heights.

7. Some Diabatic Effects

7.1 Radiative damping of acoustic gravity waves.

Golitsyn (1965) calculates that in the troposphere, the damping of waves by radiative heat transfer will be 6 orders of magnitude greater than the viscous damping, although he finds at 100 km the radiation damping will be less than viscous damping, as the viscous damping increases while radiation damping decreases somewhat with height (Golitsyn, 1963).

This numerical result is based on a simple model of gray or frequency independent absorption. Unfortunately, this model may lead to qualitatively misleading results as well as numerical inaccuracy. The expression for radiative dissipation of a temperature disturbance in a gray gas has been transformed by Goody (1964) into a form applicable to a non-gray gas. The validity of this technique for the calculation of radiative stabilization of a fluid against cellular convection has been demonstrated by Gille and

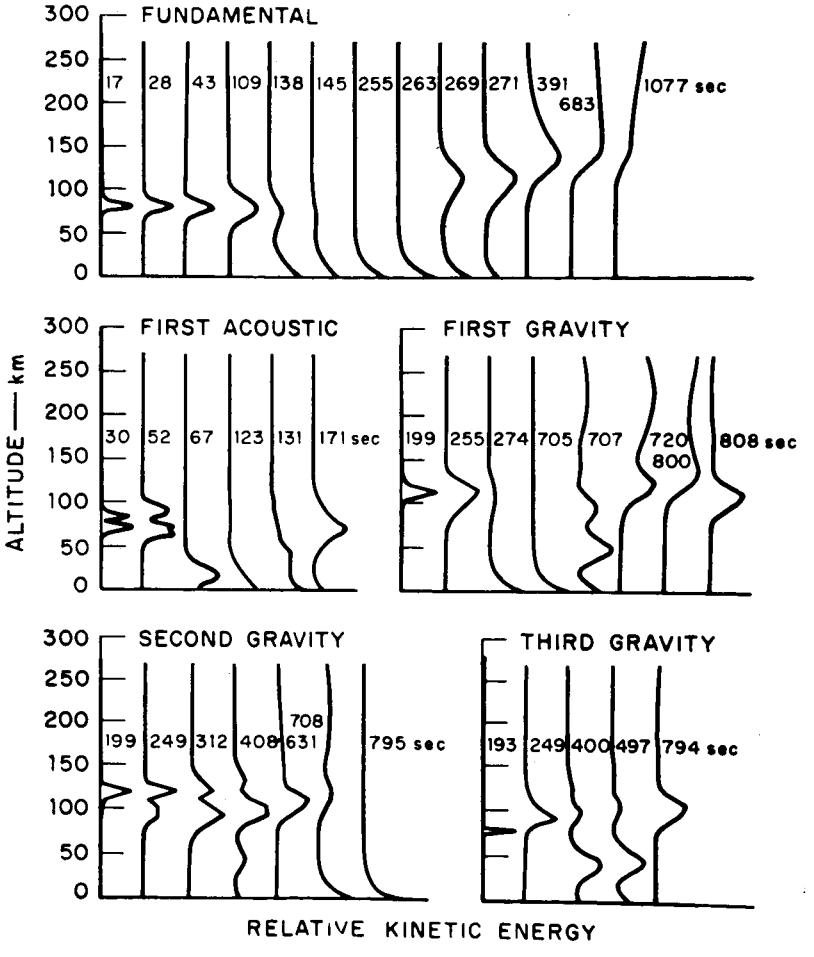

Fig. 28. Vertical profiles of relative kinetic energy in some of the lowest modes. (After Pfeffer, 1964)

Goody (1964). Quantitative studies of radiative damping in the real atmosphere should be made. Laboratory testing may also be possible.

One particularly interesting possibility is that very low frequency waves may propagate with the isothermal sound velocity, $C_T = \sqrt{RT}$ rather than the adiabatic velocity $C_s = \sqrt{\gamma RT}$.

7.2 Photochemical destabilization of gravity wave near the mesopause.

A number of recent studies, notably Leovy (1964) and Lindzen and Goody (1965), have developed linearized forms of the equations of motion in which photochemical and radiative heat sources are included. Naturally enough these involve a considerable number of drastic simplifications. Leovy (1966) has applied these ideas to gravity waves near the mesopause. If an amplification mechanism can be found, i.e., mechanism giving the waves in the mesosphere a positive growth rate, it would be nearly equivalent to putting a source in this region. A strongly attenuated wave coming up from below could have energy fed into it and amplify to observable size. If the amplification mechanism is frequency dependent, it has implications for the expected resulting spectrum.

We can see the physical basis for an amplification if we consider a column of the atmosphere displaced from its equilibrium position. If it is warmed by diabatic processes when displaced upward, it will be at a higher temperature when it comes down, and have less negative buoyancy than on the way up. Clearly, the restoring force has been reduced, and the wave amplitude will be attenuated. Here, we have a negative correlation between temperature and vertical velocity - a circumstance known in theoretical meteorology to be associated with the destruction of kinetic energy.

Conversely, if the column cools on upward displacement, its negative buoyancy is reduced, and it comes down with greater velocity through the equilibrium position than it possessed going up.

What diabatic processes might be involved? Leovy's (1966) treatment included the photochemistry of oxygen and ozone, and led to perturbation terms representing the following effects:

(1) Absorption of solar radiation by fluctuating amounts of molecular oxygen;

(2) Absorption of solar radiation by fluctuating amounts of ozone;

(3) Chemical energy released by formation of molecular oxygen and ozone from atomic oxygen.

(4) Infrared radiation.

I will merely state here the results he found, which apply to gravity waves with period 10^3 sec < P < 10^6 sec. First, since infrared radiation acts to destroy the temperature difference between the displaced column and its surroundings, destroying buoyancy, this always destroys wave energy. Second, the recombination heating and absorption of solar energy by ozone is a destabilizing effect, when the atomic oxygen mixing ratio increases with height. However, absorption by molecular oxygen is stabilizing under these circumstances.

In a numerical calculation, he finds an exponential growth rate (omitting infrared radiative effects) greater than 3×10^{-6} sec^{-1} near 90 km, for $\omega > 2.10^{-4}$ ($P \sim 1$ 1/2 hours). This indicates a doubling of amplitude in 2 1/2 days. The radiative damping is roughly calculated to be 10^{-6} sec, and eddy losses about the same for $\lambda \sim 30$ km. Damping thus will still remove all but the longest waves.

These results apply to mean conditions, and growth rates vary as the square of the atomic oxygen concentration. Since it appears that the upper winter mesosphere may be oxygen rich, this mechanism could be given a qualitative test by looking for seasonal variation of wave amplitudes and spectra in the upper mesosphere.

Certainly there are a number of very interesting ideas in this paper, and further work on these lines should be undertaken.

8. Future Problems in Wave Theory.

As is certainly clear, at present only a beginning has been made in the study of acoustic-gravity wave propagation in the atmosphere. Some important problems remaining have been discussed elsewhere - notably the effects of winds, electromagnetic forces, and non-linear interactions. The diabatic effects of radiative heating and photochemistry have been mentioned above.

There are still important problems connected with the ducting effects of temperature structure. Eckart (1960) and Weston (1961, 1962) and Pitteway and Hines (1965) have deduced general results for continous distributions

of atmospheric parameters. A number of theoretical difficulties have been lucidly set forth by Hines (1965), and although some have been answered by Pierce (1966), it appears that more work will be necessary before the nature of ducting and mode formation is fully clarified.

The effect of horizontal variations also remains for future consideration. Although velocity period curves have been calculated for different latitudes by PZ II and PH, no one has considered propagation along a path in which there are horizontal variations of temperature, heights of thermal features, topography, or wind. This is relevant to the upper atmosphere observer as well as the constructor of synthetic barograms, since energy not confined in a duct may be available to excite disturbances at E region heights. (This problem has been suggested by Pfeffer.)

In all our discussion of wave propatation, we have said very little about sources of wave energy. Until we have a clear picture of the reflection and dissipation processes in an atmosphere with winds, it will be difficult to know whether the source of energy lies in the lower atmosphere or not. It is clear that nuclear explosions, volcanic eruptions and earthquakes do create wave trains at great heights. Under what conditional meteorological disturbances in the troposphere are able to propagate energy to these heights is not clear.

A final question might be whether, by observation at the surface or with ionospheric sounding, we can obtain an atmospheric seismogram, which could then be inverted to yield information about the atmosphere or the source. J. V. Dave of the U.S. National Center for Atmospheric Research has remarked that the Umkehr method of obtaining height distribution of ozone is like unscrambling an egg. If so, we have the omlet of source, wind, and temperature to unscramble and properly reconstitute. A real start on this would not appear possible until we have better solutions to the forward problem.

Looking back at these rather large holes in our knowledge, it seems fair to say that the development of theory enabling us to handle the complexity we see in nature, and the observational search for confirmation of these theories promise to keep us supplied with challenging problems for the foreseeable future.

Acknowledgements.

The preparation of this paper was supported by NASA under grant NSG-173 and by the Florida State University. The previously unpublished diagrams of Pfeffer resulted from studies supported in part by the National Science Foundation grant NSF GP 2371 and in part by the Office of Naval Research under contract Nonr 266(70). I thank Professor Seymour Hess for his encouragement. It is a pleasure to acknowledge my debt to Professor Richard Pfeffer, who first interested me in this problem, allowed me to use unpublished material and gave me the benefit of many insights.

References

Budden, K. G., 1961: The Wave Guide Mode Theory of Wave Propagation. Englewood Cliffs, N.J., Prentice-Hall, Inc., 325 pp.

Eckart, C., 1960: Hydrodynamics of Oceans and Atmospheres. New York, Pergamon Press, 290 pp.

Gazaryan, Yu. L., 1961: Infrasonic normal modes in the atmosphere. Soviet Physics-Acoustics, 7, 17-22.

Gille, J. C., and R. M. Goody, 1964: Convection in a radiating gas. J. Fluid Mech., 20, 47-79.

Golitsyn, G. S., 1963: The influence of radiative transfer on the propagation of sound in the atmosphere. Izv., Geophys. Ser., 589-591.

_____, 1965: Damping of small oscillations in the atmosphere due to viscosity and thermal conductivity. Izv., Atmospheric and Oceanic Physics Series, 1, 82-89.

Goody, R. M., 1964: Atmospheric Radiation; I. Theoretical Basis. Oxford University Press, 436 pp.

Hines, C. O., 1965: Atmospheric gravity waves: A new toy for the wave theorist. Radio Science, 69D, 375-380.

Hunt, J. N., R. Palmer and W. Penney, 1960: Atmospheric waves caused by large explosions. Phil. Trans. Roy. Soc. A, 252, 275-315.

Lamb, H., 1945: Hydrodynamics. New York, Dover Publications, 738 pp.

Leovy, C. B., 1964: Simple models of thermally driven mesospheric circulation. J. Atmos. Sci., 21, 327-341.

_____, 1966: Photochemical destabilization of gravity waves near the mesopause. J. Atmos. Sci., 23, 223-232.

Lindzen, R. S., and R. M. Goody, 1965: The radiative-photochemical processes in mesospheric dynamics: Part I, models for radiative and photochemical processes. J. Atmos. Sci., 22, 341-348.

Pekeris, C. L., 1948: The propagation of a pulse in the atmosphere. Part II. Phys. Rev., 73, 145-154.

Pfeffer, R. L., 1962: A multi-layer model for the study of acoustic-gravity wave propagation in the earth's atmosphere. J. Atmos. Sci., 19, 251-255.

Pfeffer, R. L., 1964: Unpublished report.

Pfeffer, R. L., and J. Zarichny, 1962: Acoustic-gravity wave propagation from nuclear explosions in the earth's atmosphere. J. Atmos. Sci., 19, 256-263.

_____, 1963: Acoustic-gravity wave propagation in an atmosphere with two sound channels. Geofisica Pura a Applicata, 55, 175-199.

Pitteway, M. L. V., and C. O. Hines, 1965: The reflection and ducting of atmospheric acoustic-gravity waves. Can. J. Phys., 43, 2222-2243.

Pierce, A. D., 1966: Justification of the use of multiple isothermal layers as an approximation to the real atmosphere for acoustic-gravity wave propagation. Radio Science, 1, 265-267.

Press, F., and D. Harkrider, 1962: Propagation of acoustic-gravity waves in the atmosphere. J. Geophys. Res., 67, 3889-3908.

Scorer, R. S., 1950: The dispersion of a pressure pulse in the atmosphere. Proc. Roy. Soc., A, 201, 137-157.

Tolstoy, I., 1955a: Note on the propagation of normal modes in inhomogeneous media. J. Acoust. Soc. Am., 27, 274-277.

_____, 1955b: Dispersion and simple harmonic point sources in wave ducts. J. Acoust. Soc. Am., 27, 897-907.

_____, 1956: Resonant frequencies and high modes in layered wave guides. J. Acoust. Soc. Am., 28, 1182-1192.

_____, 1963: The theory of waves in stratified fluids including the effects of gravity and rotation. Revs. Mod. Phys., 35, 207-230.

Weston, V. H., 1961: The pressure pulse produced by a large explosion in the atmosphere. Can. J. Phys., 39, 993-1009.

_____, 1962: Gravity and acoustical waves. Can. J. Phys., 40, 446-453.